People`s Democratic Republic of Algeria

Ministry of Higher Education and Scientific Research

University of Echahid Hamma Lakhdar - El Oued

Faculty of Technology

Department of Hydraulics and Civil Engineering

PROFESSIONAL MASTER DEGREE

Specialty: Design and diagnosis of drinking water supply and sanitation systems

Presented by:

1. DEBBAR Oumaima

2. AOUIN Mohammed Salah

Entitled:

Generalized Neural Network for Precise Evapotranspiration Estimation: A Solution for Water-Scarce Agriculture in Mila, Algeria

Dissertation Submitted in Partial Fulfillment of the Requirements for the Master Degree in Master's

Publicly defended in: 27/06 /2025

Board of Examiners:

Dr. KHEZAZNA Amina	**Chairman**
Dr. MEZIANI Assia	**Supervisor**
Dr. ZAIZ Issam	**Examiner**

university Year: 2024/2025

Abstract

This research addresses the growing challenge of water scarcity in Mila, Algeria, and its impact on agricultural sustainability. The primary objective is to develop a robust and accurate model for estimating reference evapotranspiration (ET_0), a critical variable for irrigation planning. The study employs a Generalized Regression Neural Network (GRNN) model, trained on limited climatic data, and uses the FAO Penman-Monteith method as a benchmark for validation. The methodology involved data collection from 2000 to 2024, model training with a three-way data split (training, validation, testing), and performance evaluation using statistical metrics including RMSE, MAE, R^2, NSE, and Willmott's index. Results indicate that the GRNN model achieved excellent predictive performance ($R^2 \approx 0.96$, RMSE < 0.4), demonstrating its ability to generalize well and operate effectively under data-scarce conditions. This confirms the potential of machine learning models to support smart irrigation strategies and enhance water use efficiency in semi-arid regions.

Keywords:

Reference evapotranspiration, GRNN, Machine learning, irrigation management, water scarcity.

ملخص

يتناول هذا البحث مشكلة شح المياه المتزايدة في ولاية ميلة بالجزائر وتأثيرها المباشر على استدامة الزراعة. يهدف العمل أساسًا إلى تطوير نموذج دقيق وفعّال لتقدير التبخر-النتح المرجعي(ET_0) ، باعتباره عنصراً أساسياً في تخطيط الري. تم اعتماد نموذج الشبكة العصبية الانحدارية المعممة(GRNN) ، الذي تم تدريبه باستخدام بيانات مناخية محدودة، مع اعتماد معادلة بنمان-مونتيث الصادرة عن منظمة الفاو كمرجع للمقارنة. شملت المنهجية جمع بيانات مناخية للفترة الممتدة من 2000 إلى 2024، وتقسيم البيانات إلى ثلاث مجموعات (تدريب، تحقق، اختبار)، وتقييم أداء النموذج باستخدام مؤشرات إحصائية مثل RMSE و MAEو R^2و NSEومؤشر الاتفاق لويلموت. أظهرت النتائج أن النموذج حقق أداءً تنبؤياً ممتازاً ($R^2 \approx 0.96$) و(RMSE < 0.4، مما يبرز قدرته على التعميم والعمل بكفاءة في ظل محدودية البيانات. تؤكد هذه النتائج فعالية استخدام نماذج الذكاء الاصطناعي في دعم استراتيجيات الري الذكي وتعزيز كفاءة استعمال المياه في المناطق شبه الجافة.

الكلمات المفتاحية:

التبخر-النتح المرجعي، GRNN، **تعلم الآلة**، إدارة الري، شح المياه.

Résumé

Cette étude traite du problème croissant de la rareté de l'eau à Mila, en Algérie, et de ses répercussions sur la durabilité de l'agriculture. L'objectif principal est de développer un modèle fiable et précis pour estimer l'évapotranspiration de référence (ET_0), une variable essentielle pour la planification de l'irrigation. Un modèle de réseau neuronal à régression généralisée (GRNN) a été élaboré à partir de données climatiques limitées, avec la méthode de Penman-Monteith de la FAO utilisée comme référence pour la validation. Les données climatiques couvrant la période de 2000 à 2024 ont été utilisées, avec une division en trois sous-ensembles : entraînement, validation et test. Les performances du modèle ont été évaluées à l'aide de plusieurs indicateurs statistiques, notamment le RMSE, le MAE, le R^2, le NSE et l'indice de Willmott. Le modèle GRNN a démontré une excellente précision prédictive ($R^2 \approx 0,96$; RMSE < 0,4), confirmant sa capacité à généraliser efficacement, même en conditions de données limitées. Ces résultats soulignent le potentiel des approches d'apprentissage automatique pour soutenir une gestion intelligente de l'irrigation et améliorer l'efficacité de l'utilisation de l'eau dans les régions semi-arides.

Mots-clés : Évapotranspiration de référence, GRNN, Apprentissage automatique, Gestion de l'irrigation, Rareté de l'eau.

Thanks

We begin by expressing our deepest gratitude to **Allah Almighty**, whose guidance and blessings have enabled us to complete this humble work.

We extend our sincere thanks and profound respect to everyone who supported us, whether directly or indirectly, throughout this journey.

In particular, we are especially grateful to **Dr. MEZIANI Assia** for her unwavering support, invaluable advice, and the confidence she instilled in us. Her generosity in sharing her expertise and experience was instrumental in the realization of this work.

We would also like to express our heartfelt appreciation to the esteemed **jury members** for kindly accepting to be part of this honorable committee and for dedicating their time and attention to our work.

Finally, we extend our sincere thanks to our colleagues and all our respected teachers, whose guidance and encouragement have been a source of strength throughout our academic journey.

الإهداء

﴿ وَقُلِ اعْمَلُوا فَسَيَرَى اللَّهُ عَمَلَكُمْ وَرَسُولُهُ وَالْمُؤْمِنُونَ ۖ وَسَتُرَدُّونَ إِلَىٰ عَالِمِ الْغَيْبِ وَالشَّهَادَةِ فَيُنَبِّئُكُم بِمَا كُنتُمْ تَعْمَلُونَ ﴾

[التوبة: 105]

(من قال أنا لها نالها)

الحمد لله حبا وشكرا وامتنان الذي بفضله هأنا اليوم أنضر الى حلم طال إنتظاره وقد أصبح واقعا أفتخر به

أهدي هذا النجاح إلى نفسي الطموحة أ ولا ابتدأت بطموح وانتهت بنجاح

إلى ملاكي الطاهر وقوتي بعد الله داعمتي الأولى والابدية أمي أهديكي هذا الإنجاز الذي لولا تضحياتك لما كان له وجود ممتنة لان الله قد اصطفاك لي من البشر

أما يا خير سند وعوض الى النور الذي أنار دربي والسراج الذي لا ينطفئ نوره والذي بذل جهد السنين من أجل أن أعتلي سلالم النجاح إلى والدي العزيز

الى ترابها الطاهر وإلى من هم أفضل منا في بقاعي هذه الأرض إلى شهدائها أطفالا وكبار ومجهديها الابطال الى من يموتون في سبيل البلاد والمقدسات والدين الإسلام إلى غزة اللهم النصر القريب

Tables of contents

List of figures

List of tables

List of Abbreviations

FAO	Food and Agriculture Organization
ET_0	Reference Evapotranspiration
PM	Penman-Monteith Model
GRNN	Generalized Regression Neural Network
ANN	Artificial Neural Network
R^2	Coefficient of Determination
RMSE	Root Mean Square Error
MAE	Mean Absolute Error
NSE	Nash-Sutcliffe Efficiency
WILSR	Willmott's Index of Agreement
RSR	RMSE to Standard Deviation Ratio
Tmean	Mean Temperature
Tmin	Minimum Temperature
Tmax	Maximum Temperature
RH	Relative Humidity
Rs	Solar Radiation
U_2	Wind Speed at 2 meters height
P	Precipitation

General Introduction

General Introduction

Water scarcity is an increasingly pressing concern worldwide, particularly in arid and semi-arid regions that face persistent limitations in water resources. Agriculture is one of the largest consumers of freshwater, accounting for approximately **70%** of global freshwater withdrawals. This makes efficient water management crucial for achieving agricultural sustainability and meeting the needs of a growing population.

Evapotranspiration (ET) is a key component of the agricultural water cycle, representing the combined loss of water through evaporation from the soil and transpiration from plant leaves. Accurate estimation of ET rates is essential for improving water use efficiency in irrigation practices and reducing waste, thereby enhancing agricultural productivity and ensuring sustainable use of natural resources.

Traditional methods for estimating evapotranspiration, such as the **Penman-Monteith equation,** require extensive and detailed climatic data, including temperature, humidity, wind speed, and solar radiation. However, these methods may lack accuracy under varying local environmental conditions or when complete data is unavailable.

In **Mila, Algeria,** where agriculture faces significant challenges due to water scarcity, there is an urgent need for more precise ET estimation techniques to develop more efficient irrigation strategies. Inaccurate ET estimates can lead to either water wastage or insufficient irrigation, negatively impacting crop yields and agricultural productivity.

In light of these challenges, **Artificial Intelligence (AI) technologies** have emerged as a promising solution to enhance the accuracy of evapotranspiration estimation. Among these technologies, **Generalized Neural Networks (GNNs)** stand out as a powerful tool, capable of effectively handling the complex nonlinear relationships between various climatic variables. By leveraging GNNs, it is possible to develop models that significantly improve the precision of evapotranspiration predictions. This, in turn, leads to more efficient water use and reduces wastage, thereby supporting sustainable agricultural practices and addressing the critical issue of water scarcity in arid and semi-arid regions.

The ability of GNNs to learn from historical data and adapt to local environmental conditions makes them an ideal choice for developing robust and accurate evapotranspiration estimation models, particularly in areas like Mila, Algeria, where water resources are limited and precise management is essential for agricultural productivity.

- Geographical and Climatic Characteristics of Mila Region
- Artificial Intelligence Methods vs. Classical Approaches: A Review in Evapotranspiration Estimation"

- Development of a(GNN) Model for Accurate (Et) Estimation and Its Performance Evaluation

Chapter I: Geographical and Climatical Characteristics of Mila Region

I.1.Introduction

Mila Province, located in north-eastern Algeria, faces mounting agricultural challenges due to climate change and persistent water scarcity. This chapter outlines the region's geographic and climatic context, supported by monthly data from 2000 to 2024. Emphasis is placed on critical parameters such as temperature, precipitation, humidity, and soil moisture, which collectively influence crop water requirements. Moreover, the chapter identifies the primary water sources—including rivers, dams, and groundwater—and highlights the adverse impact of poor water management on agricultural productivity. Understanding these environmental constraints is essential for developing efficient irrigation strategies tailored to local conditions.

I.2. Study Area:

Mila Province is situated approximately between 36.45° N latitude and 6.26° E longitude, locale in the north-eastern part of Algeria. It has a population of approximately 1 million (according to recent estimates) and covers an area of about 9,375 square kilometres. The capital of the province is the city of Mila, and it is situated near the provinces of Jijel, Constantine, Oum El Bouaghi, and Skikda, which enhances its strategic location. The province is characterized by its diverse geography, including mountains, fertile plains, and forests, making it an important agricultural region that produces cereals, olives, and fruits. Its climate is Mediterranean, with hot, dry summers and mild, rainy winters [1].

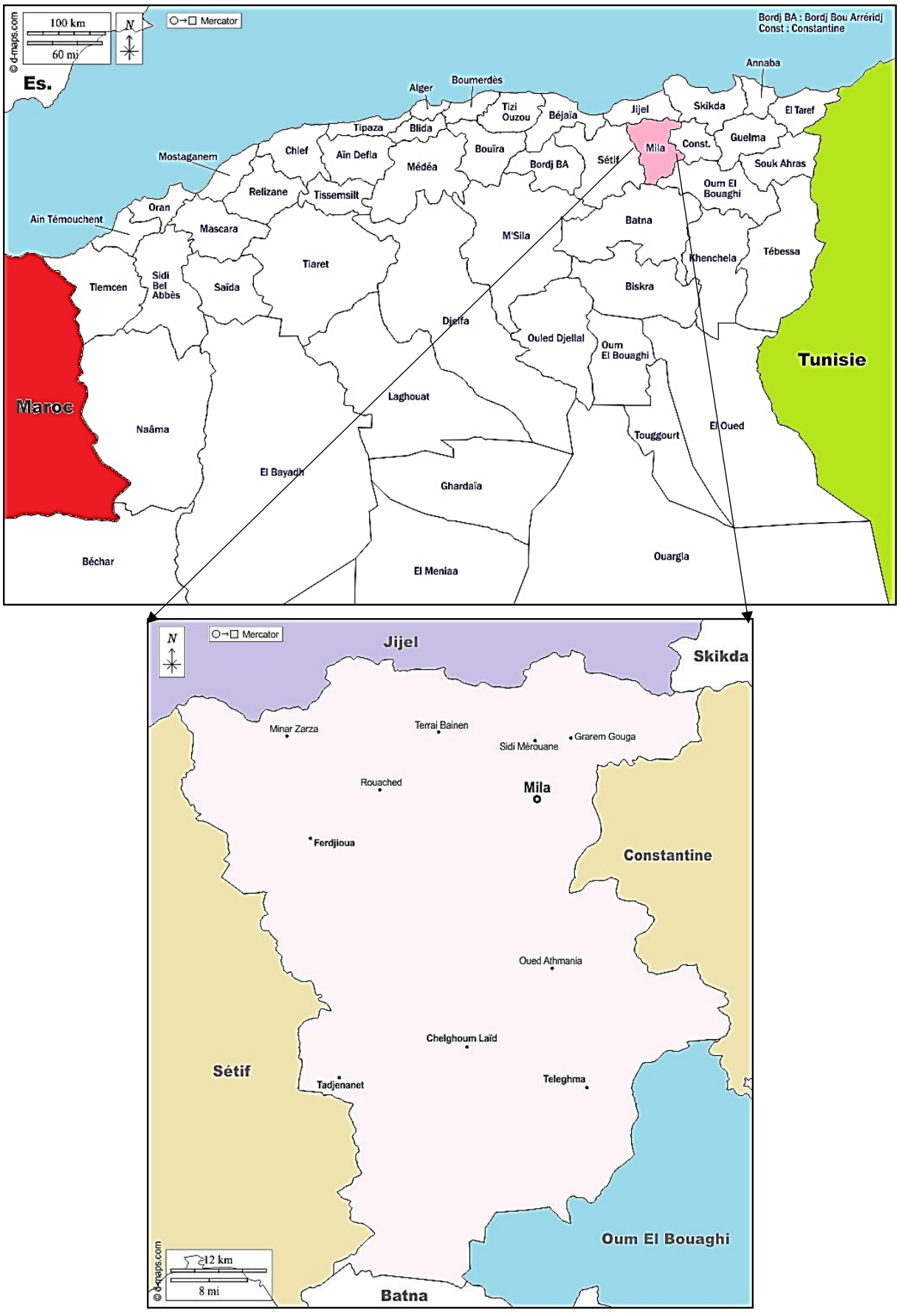

Figure I-1: Illustrative map of the Mila area [2].

Mila Province, located in north-eastern Algeria, is distinguished by a rich and varied physical geography. The northern part of the province forms a segment of the Tell Atlas Mountains, contributing to its topographical complexity and offering natural barriers that shape local ecosystems. To the south, the terrain transitions into fertile plains, which are extensively utilized for cereal agriculture due to their favourable soil and climatic conditions. Additionally, parts of the province are covered by dense forest vegetation, which enhances regional biodiversity and serves as a critical environmental resource. Several rivers, notably the Rhumel and El Kebir, traverse the area and play a vital role in sustaining irrigation systems and agricultural productivity. Geopolitically, Mila's central location—bordering Jijel to the north, Constantine to the east, Oum El Bouaghi to the south, and Skikda to the northeast—facilitates its function as a logistical and commercial hub in the north-eastern corridor of Algeria [3] [4].

I.2.1. Climate:

The climate of Mila Province exhibits the typical features of the Mediterranean climatic zone. Summers are characteristically hot and dry, with daytime temperatures frequently surpassing 30°C during the peak months of July and August. In contrast, winters are mild and relatively wet, with average temperatures ranging around 10°C, and precipitation largely concentrated between November and March. This seasonal distribution of rainfall significantly influences both natural vegetation cycles and agricultural practices. While the climate offers opportunities for the cultivation of a variety of crops, it also necessitates adaptive management, particularly in response to interannual variability in precipitation [**6**].

I.2.2 Agriculture:

Agriculture remains one of the cornerstones of Mila Province's economy, underpinned by favorable natural conditions and traditional expertise. The region is especially notable for its cereal production, including both wheat and barley, which dominate agricultural output. Olive cultivation is another prominent feature of the province's agrarian identity, with extensive groves supporting both local consumption and commercial olive oil production. Fruit agriculture is also significant, encompassing citrus fruits, figs, and grapes. Despite these strengths, the sector faces notable challenges, including rugged topography in some zones and climatic constraints such as seasonal droughts, which impact productivity and the effective use of land resources [3] [4].

I.3. Regional Climate Data (2000–2024):

I.3.1. Precipitation:

The precipitation data indicates a clear seasonal variation, The monthly system for the Mila region during the period 2000-2024 is shown, the highest values recorded in winter months such as November (2.89 mm) and the lowest in summer months like July (0.1 mm) The rainfall pattern shows concentration in autumn and winter, while summer months are relatively dry. The annual average precipitation is approximately 1.8 mm, suggesting an arid climate with significant monthly fluctuations

Table I-1: Average annual precipitation from 2000 to 2024[5]

month	J	F	M	A	M	J	J	A	S	O	N	D
Precipitation (mm)	2,8	3	2,6	2,59	1,95	0,62	0,1	0,49	1,56	2,05	2,89	2,86

Figure I-2: Average ANNUAL PRECIPITATION FROM 2000 to 2024[5]

I.3.2. Air temperature (Same thing for others):

The monthly temperature pattern recorded in Mila Province during the period 2000-2024 indicates that the lowest monthly temperature was recorded in January, reaching 7.52°C, while the highest recorded temperature was 27.3°C in July.

Table I-2: Average annual temperature from 2000 to 2024[5]

Month	Jan	Feb	Mar	Apr	May	Jun	Jul	Aug	Sep	Oct	Nov	Dec
Air Temperature at 2m (°C)	7,52	8,28	11,07	14	17,94	23,27	27,3	26,79	22,63	18,44	12,5	8,75

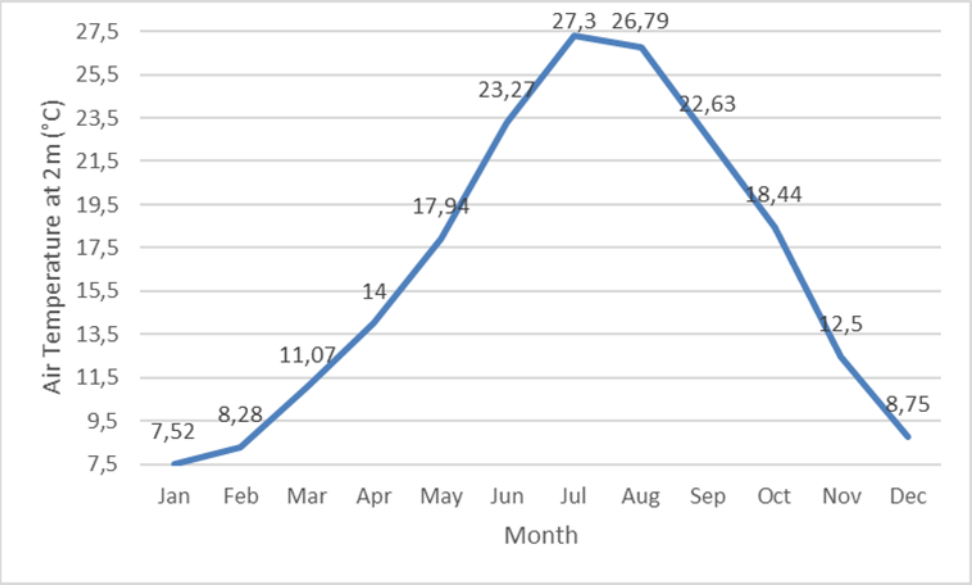

Figure I-3: Average annual temperature from 2000 to 2024[5]

I.3.3. Relative Humidity:

The relative humidity pattern across the 2000–2024 period reveals inverse seasonality relative to temperature and solar radiation. The most humid conditions occur in winter, with a peak in December (78.32%), whereas July records the driest atmosphere (47.18%). These findings reflect the interplay of temperature, moisture availability, and atmospheric saturation capacity.

Table I-3: Average annual Relative Humidity from 2000 to 2024[5]

Month	Jan	Feb	Mar	Apr	May	Jun	Jul	Aug	Sep	Oct	Nov	Dec
Relative Humidity (%)	77.98	76.46	74.57	72.80	68.41	57.17	47.18	50.90	62.84	67.22	73.26	78.32

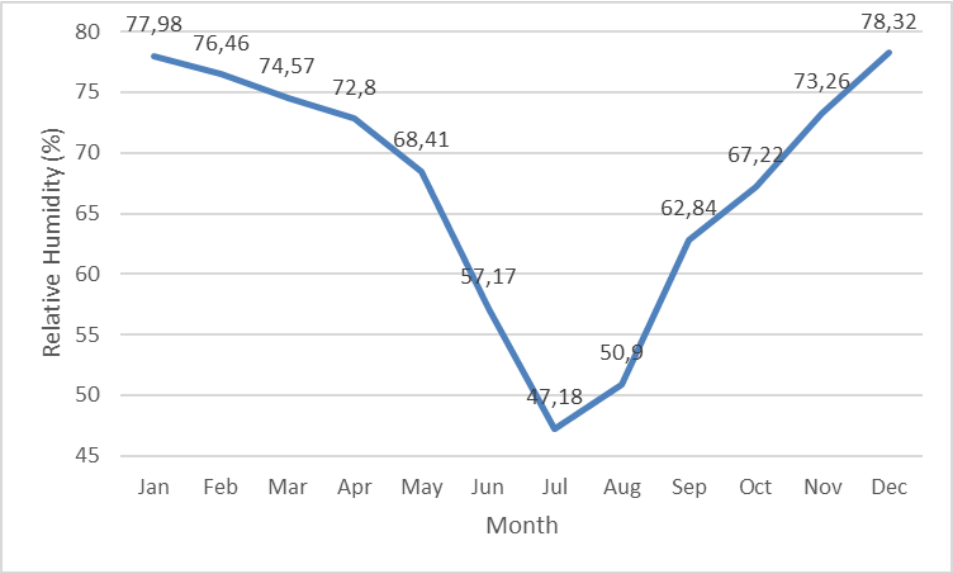

Figure I-4: Average annual Relative Humidity from 2000 to 2024 [5]

I.3.4.Wind Speed:

Wind speed at 10 meters above ground shows slight variability throughout the year across the 2000–2024 timeframe. The windiest months occur during late winter and early spring, with February reaching 7.64 km/h. Speeds decline slightly into summer, with the lowest average in September (6.06 km/h), likely due to more stable atmospheric conditions. The overall pattern suggests moderate winds, with seasonal influences linked to pressure gradients and topographical effects.

Table I- 4: Average annual Wind speed from 2000 to 2024[5]

Month	Jan	Feb	Mar	Apr	May	Jun	Jul	Aug	Sep	Oct	Nov	Dec
Wind Speed at10m (km/h)	7,46	7,64	7,39	7,04	6,62	6,4	6,51	6,28	6,06	6,08	7,06	7,11

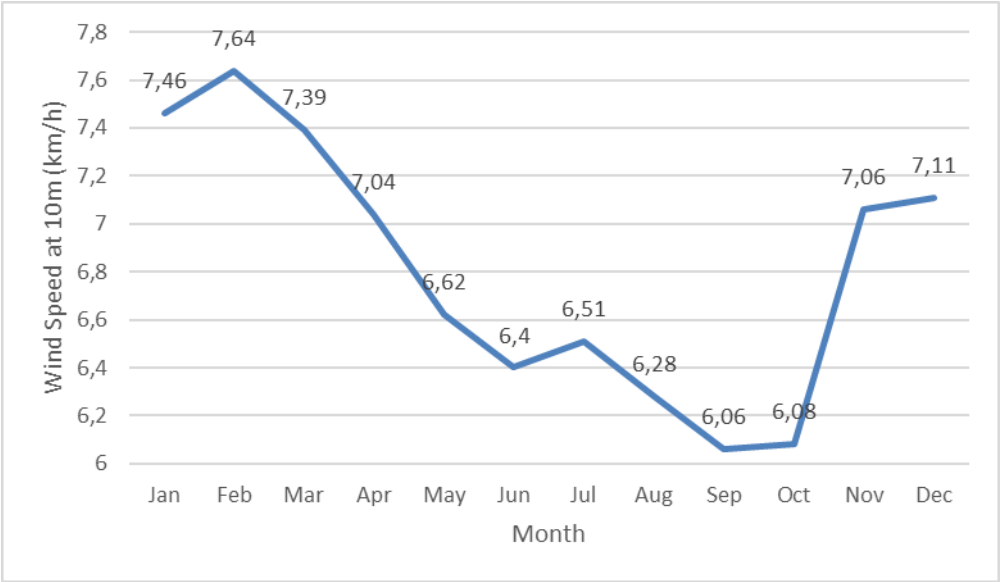

Figure I-5: Average annual WIND SPEED FROM 2000 TO 2024[5]

I.3.5. Soil Moisture:

Throughout the 2000–2024 timeframe, soil moisture in the top 0–7 cm layer displays a distinct seasonal rhythm. Moisture levels peak in winter, particularly in February (0.34 m^3/m^3), and decline steadily through spring and early summer, reaching a minimum in July (0.14 m^3/m^3). This trend corresponds with increased evapotranspiration and reduced precipitation during hotter months, illustrating a marked soil desiccation in summer.

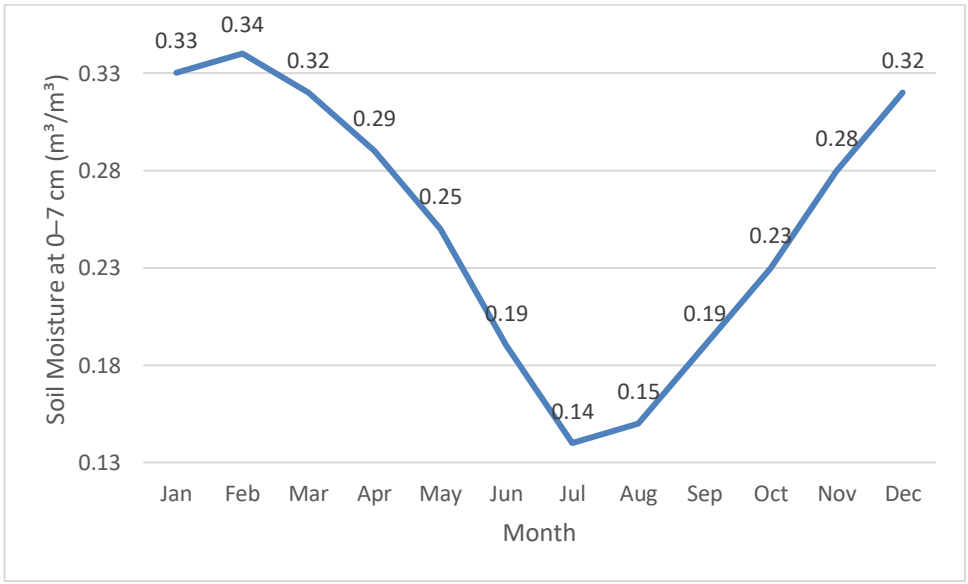

Figure I-6: Average annual Soil moisture from 2000 to 2024[5]

Table I-5: Average annual soil moisture from 2000 to 2024[5]

Month	Jan	Feb	Mar	Apr	May	Jun	Jul	Aug	Sep	Oct	Nov	Dec
Soil Moisture at 0–7 cm (m^3/m^3)	0,33	0,34	0,32	0,29	0,25	0,19	0,14	0,15	0,19	0,23	0,28	0,32

I.3.6. Dew Point:

Analysis of dew point data from 2000 to 2024 shows a progressive rise from winter into late summer, with the highest value recorded in September (13.80°C) and the lowest in January (3.47°C). These variations mirror seasonal changes in atmospheric humidity, with elevated dew point values during the warm season reflecting higher moisture retention in the air.

Table I-6 : Average annual dew point from 2000 to 2024[5]

Month	Jan	Feb	Mar	Apr	May	Jun	Jul	Aug	Sep	Oct	Nov	Dec
Dew Point at 2m (°C)	3,47	3,81	6,04	8,43	11	12,64	13,06	13,71	13,8	11,07	7,15	4,76

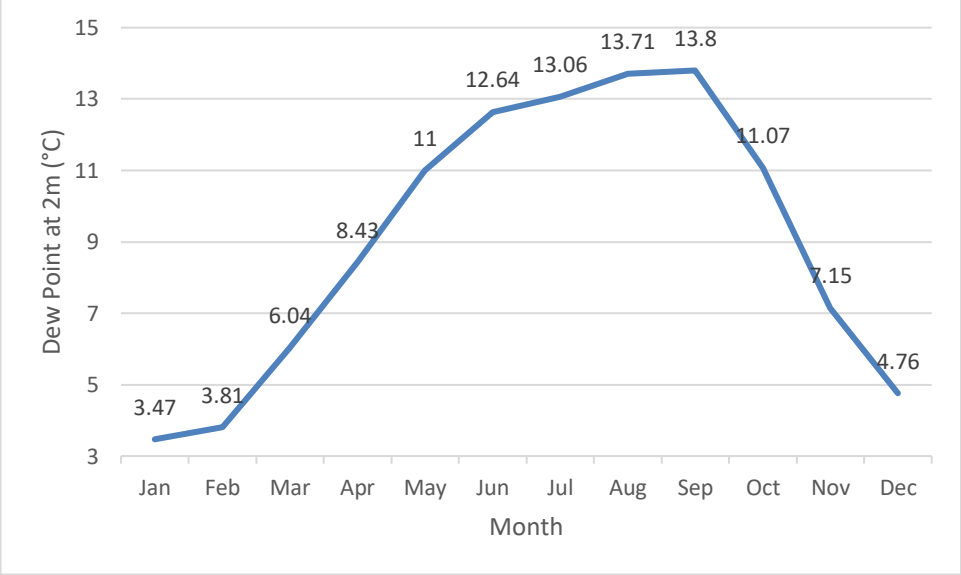

Figure I-7: Average annual dew point from 2000 to 2024[5]

I.3.7. Soil Temperature:

Over the course of the 2000–2024 period, soil temperature measurements indicate a smooth seasonal cycle. The coldest values occur in January (7.59°C), rising progressively to a summer maximum in July (29.39°C). This warming trend closely follows solar radiation input

and air temperature fluctuations, emphasizing the shallow soil layer's sensitivity to surface climate conditions.

Table I-7: Average annual soil temperature from 2000 to 2024[5]

Month	Jan	Feb	Mar	Apr	May	Jun	Jul	Aug	Sep	Oct	Nov	Dec
Soil Temperature at 0–7 cm (°C)	7,59	8,58	11,44	14,78	19,02	24,69	29,39	28,99	24,4	19,38	13,07	8,94

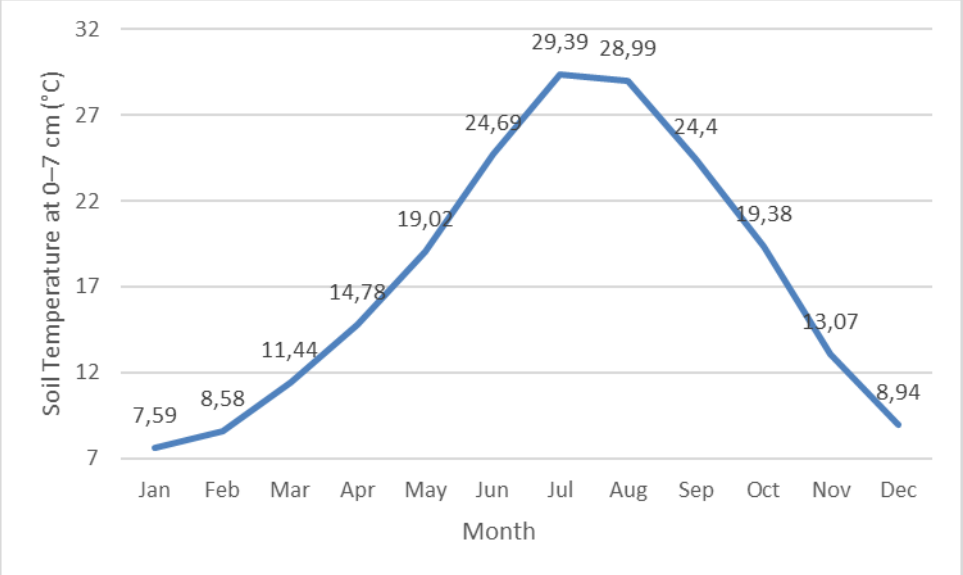

Figure I-8: Average annual soil temperature from 2000 to 2024[5]

I.3.8. Sunshine Duration:

The sunshine duration data from 2000 to 2024 highlight significant intra-annual variability. Maximum sunlight hours are concentrated in the summer months—especially July (37096.19 s)—while the shortest durations are noted in December (21875.55 s). These patterns are consistent with daylength and cloud cover variations across the seasons, influencing both temperature and evaporation.

Table I-8: Average annual sunshine duration from 2000 to 2024[5]

Month	Jan	Feb	Mar	Apr	May	Jun	Jul	Aug	Sep	Oct	Nov	Dec
Sunshine Duration (s)	22388,62	25306,2	28040,4	30937,88	33065,62	36390,13	37096,19	34849,35	29708,25	26542,19	22692,84	21875,55

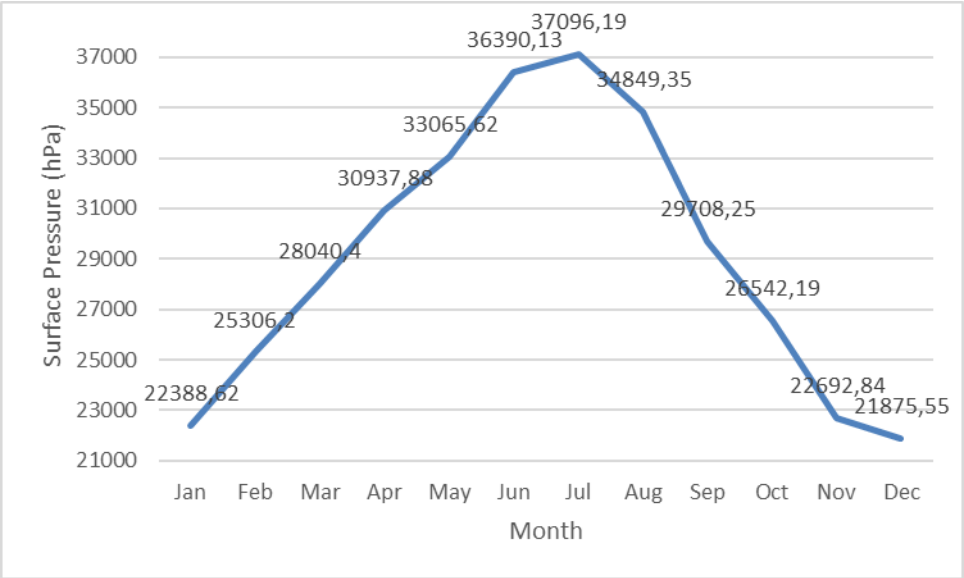

Figure I-9: Average annual sunshine duration from 2000 to 2024[5]

I.3.9. Surface Pressure:

Examining atmospheric pressure trends between 2000 and 2024 reveals only minor monthly variation. The pressure reaches its lowest point in April (960.65 hPa), while December (965.43 hPa) and January (965.27 hPa) exhibit the highest values. This modest fluctuation suggests a relatively stable pressure environment throughout the year, with subtle shifts likely influenced by regional circulation systems.

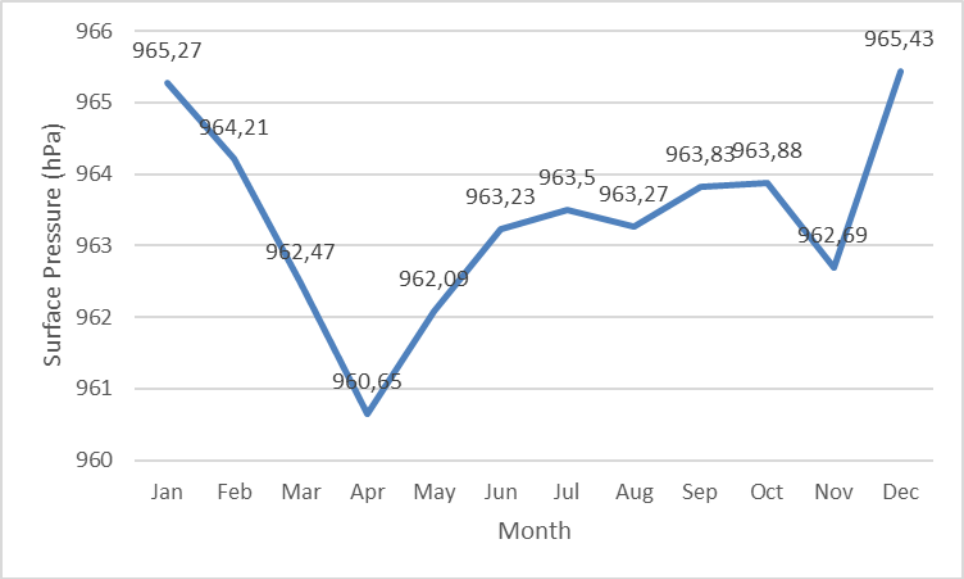

Figure I-10: Average annual Surface Pressure from 2000 to 2024[5]

Table I-9: Average annual Surface Pressure from 2000 to 2024[5]

Month	Jan	Feb	Mar	Apr	May	Jun	Jul	Aug	Sep	Oct	Nov	Dec
Surface Pressure (hPa)	965, 27	964, 21	962, 47	960, 65	962, 09	963, 23	963 ,5	963, 27	963, 83	963, 88	962, 69	965, 43

I.3.10. Terrestrial Radiation

Monthly averages of terrestrial radiation during 2000–2024 display a seasonal profile, beginning at lower levels in January (204.79 W/m²) and steadily increasing to a peak in June (483.52 W/m²). Radiation then declines into winter, paralleling solar altitude and daylength changes. The summer maximum is indicative of strong surface heating under high insolation.

Table I-10: Average annual terrestrial radiation from 2000 to 2024[5]

Month	Jan	Feb	Mar	Apr	May	Jun	Jul	Aug	Sep	Oct	Nov	Dec
Terrestrial Radiation (W/m²)	204, 79	264, 98	343, 34	415, 63	465, 34	483, 52	471, 98	430, 42	366, 34	287, 95	219, 79	186 ,6

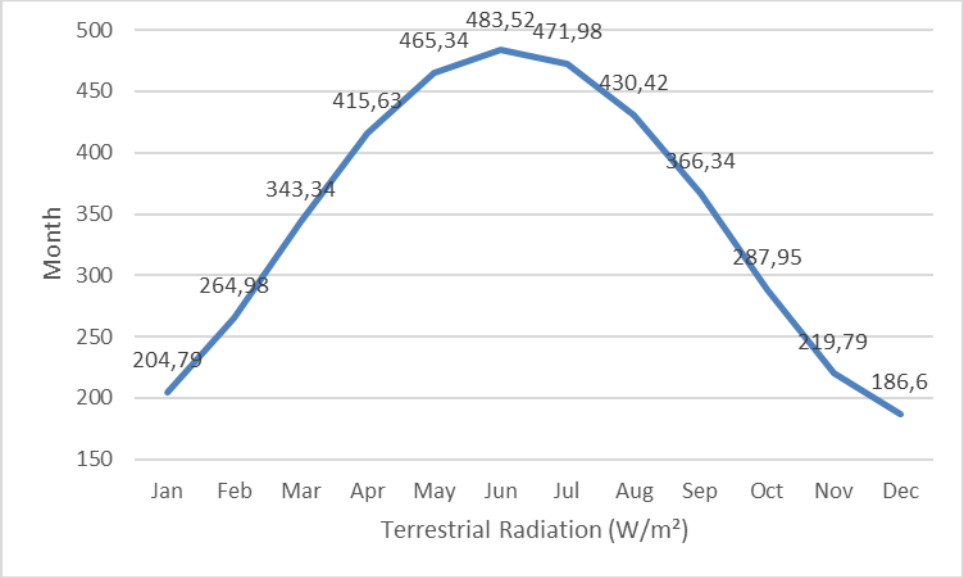

Figure I-11: Average annual terrestrial radiation from 2000 to 2024[5]

I.3.11. Vapor Pressure:

The vapor pressure deficit (VPD) illustrates an ascending gradient from winter into summer, culminating in July (2.31 kPa), and declining thereafter. January and December record the lowest VPD values, around 0.3 kPa. High summer VPD values imply intense atmospheric demand for moisture, highlighting a strong potential for plant water stress in dry months.

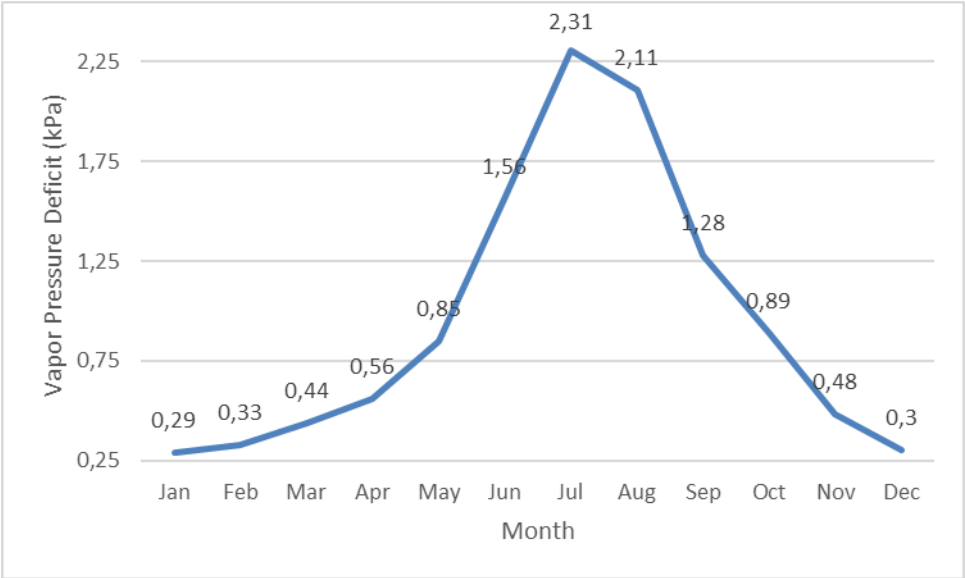

Figure I-12: Average annual vapor pressure from 2000 to 2024[5]

Table I-11: Average annual vapor pressure from 2000 to 2024[5]

Month	Jan	Feb	Mar	Apr	May	Jun	Jul	Aug	Sep	Oct	Nov	Dec
Vapor Pressure Deficit (kPa)	0,29	0,33	0,44	0,56	0,85	1,56	2,31	2,11	1,28	0,89	0,48	0,3

I.4.Water Resources:

Water resources in the **Mila region**, located in north-eastern Algeria, are vital for agricultural and economic development. However, these resources are under significant pressure due to **climate change** and **poor management**, making their study essential to understanding the challenges facing the region.

I.4.1. Main Sources:

a) Rivers

Mila relies on several major rivers, including Oued El Kebir and Oued Rhumel, which are important sources of surface water. These rivers provide a significant portion of the water used for irrigation and drinking, especially during the rainy seasons.

b) Dams

The region's main dams include the Beni Haroun Dam, one of the largest dams in Algeria, with a storage capacity of [insert data] million cubic meters. Additionally, the Oued Zhour Dam contributes to supplying water for agriculture and domestic use.

c) Groundwater

The region also depends on groundwater, extracted from wells However, overexploitation of these resources has led to a decline in water tables, threatening their long-term sustainability.

d) Water Scarcity

The Mila region suffers from **water scarcity** due to declining rainfall rates in recent years, attributed to climate change. Additionally, poor water resource management, such as leaks in distribution networks and inefficient water use, exacerbates the problem.

I.4.2. Impact of Water Scarcity on Agriculture:

Water scarcity has led to a decline in agricultural productivity, as farmers heavily rely on irrigation. Crops such as **wheat** and **olives** are threatened by water shortages, impacting food security and the local economy. Reduced crop yields also result in significant economic losses for farmers. [7]

I.5.Conclusion

The Mila region, located in north-eastern Algeria, represents a key agricultural zone constrained by increasing water scarcity and climatic variability. Analysis of climate data from 2000 to 2024 reveals a clear pattern of low annual precipitation (≈1.8 mm) concentrated in winter, with hot, dry summers and rising temperatures exceeding 27°C in July. Soil moisture, dew point, and vapor pressure data further reflect increasing atmospheric dryness during the summer period, intensifying crop water demand.

In addition to climate stressors, inefficient water resource management and groundwater overexploitation have worsened the impact of drought conditions. The region's agricultural productivity—especially cereal and olive cultivation—is highly vulnerable. These findings underscore the urgent need for more precise irrigation planning and adaptive water management tools suited to arid environments like Mila.

Chapter II: Machine Learning Methods vs. Classical Approaches: A Review in Evapotranspiration Estimation

II.1.Introduction

Evapotranspiration (ET_0) is a core variable in irrigation scheduling and water resource planning. Classical models like the FAO Penman-Monteith equation offer scientifically validated methods but rely on comprehensive meteorological datasets. In contrast, machine learning approaches—especially neural networks—can estimate ET_0 under incomplete data conditions with high accuracy. This chapter presents a comparative analysis of physical and AI-based models, focusing on their principles, input requirements, strengths, and limitations. It sets the theoretical foundation for selecting GRNN as the modelling tool of choice, due to its ability to model complex, nonlinear climate interactions relevant to semi-arid agriculture.

II.2. The concept of evapotranspiration:

Evapotranspiration (ET) is a critical natural process that links the water cycle to plant growth and climatic conditions. It represents the **total water loss** from the land surface to the atmosphere, resulting from **two concurrent mechanisms**: evaporation and transpiration.

Evaporation refers to the physical transformation of liquid water into water vapor from open surfaces such as soil, water bodies, and wet vegetation. This process is mainly driven by solar radiation and atmospheric demand, and it is influenced by factors such as air temperature, wind speed, and relative humidity. When water availability at the surface is sufficient, evaporation is controlled primarily by weather conditions. However, in dry soils or during extended dry periods, the limitation shifts toward the soil's ability to supply moisture to the surface.

On the other hand, **transpiration** involves the biological release of water vapor through the stomata of plant leaves. It is a physiological process regulated by the plant, as roots absorb water from the soil and transport it upward to the leaves, where it eventually evaporates into the atmosphere. Transpiration is similarly influenced by climatic factors but is also affected by crop type, growth stage, soil moisture availability, and overall plant health.

Since both processes occur simultaneously in cultivated fields, particularly during the crop growing season, they are generally considered together under the term **evapotranspiration**. In early stages of plant development, soil evaporation tends to dominate due to limited canopy coverage. As the crop grows and shades the ground, transpiration becomes the predominant component of ET. Understanding this dynamic is essential for estimating water requirements in agriculture, especially in water-limited regions. [8]

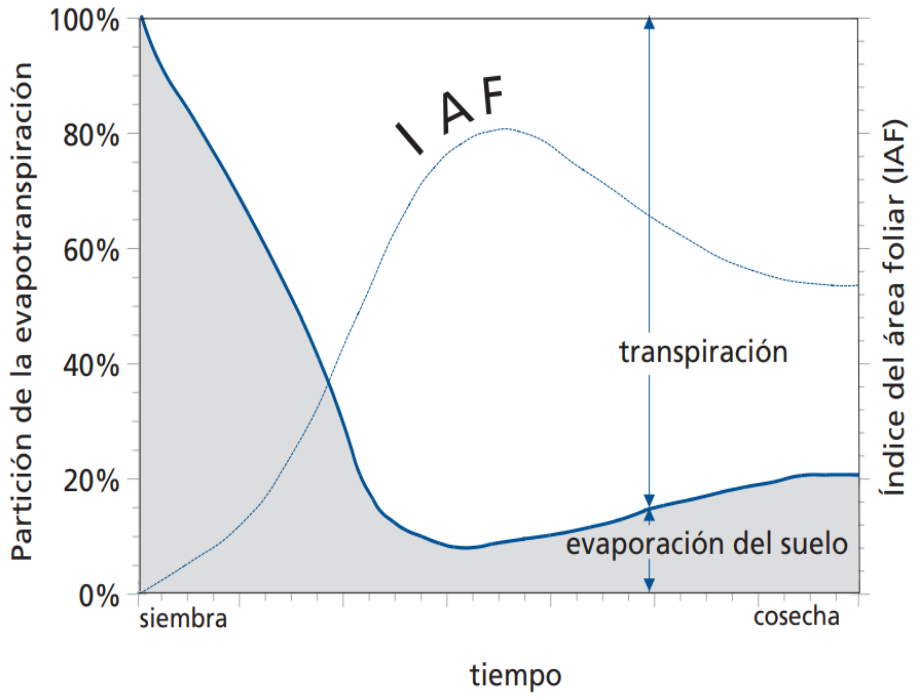

Figure II.:1 Partitioning of evapotranspiration into evaporation and transpiration during the growth period of an annual crop **[8]**

II.3. Models for Estimating Reference Evapotranspiration (ET_0)

II.3.1. Traditional Physical Models:

Over the past several decades, researchers and practitioners have developed a variety of empirical models to estimate reference evapotranspiration (ET_0) based on climatic variables. While these methods have played a crucial role in water management for agriculture, their performance has often varied depending on the region and local conditions. Most of these methods are based on local calibration and, therefore, lack universal applicability. Consequently, testing the accuracy of these models under different climatic conditions can be labour-intensive, time-consuming, and costly.

To address this challenge, the Food and Agriculture Organization (FAO) issued guidelines in their **Irrigation and Drainage Paper No. 24**, which recommended four primary methods for calculating reference crop evapotranspiration (ET_0). These methods were designed to accommodate varying levels of data availability:

1. **Blaney-Criddle Method** – This method relies solely onair temperature data and is suitable for regions with limited climatic information.

2. **Radiation Method** – Recommended for locations where data such as solar radiation or sunshine duration are available, but where wind speed and humidity data are not accessible.
3. **Modified Penman Method** – Considered to produce the most accurate estimates for reference grass crops, this method has limitations and tends to overestimate ET_0, particularly under conditions of low evaporation.
4. **Pan Evaporation Method** – This method uses evaporation measurements from a standard pan, providing estimates that can be accurate depending on the pan's location and maintenance.

- Each of these methods was designed to be applied at different time intervals: the **Blaney-Criddle method** was intended for monthly calculations, while the **pan evaporation method** was better suited for 10-day or longer intervals. However, these guidelines were frequently overlooked by practitioners who applied these methods at daily scales, leading to inaccuracies in estimation.

Despite their widespread use, these traditional methods have shown limitations. Studies evaluating their performance across various climates revealed that they do not always align with observed values of ET_0, with some methods overestimating or underestimating evapotranspiration, particularly in arid or humid conditions. For example, the **modified Penman method** consistently overestimated ET_0 by up to 20% in low-evaporation conditions. Meanwhile, the **pan evaporation method** showed variable accuracy, depending on local climatic factors and maintenance practices.

These inconsistencies highlighted the need for a standardized method of estimating ET_0 that could perform reliably across different regions. The **FAO Penman-Monteith method** emerged as the preferred solution, offering more accurate and consistent results across diverse climates, even when limited data is available. Therefore, the use of older FAO ET methods or alternative reference ET approaches is now generally discouraged.

II.3.1.1. The Penman-Monteith Model

Efficient water management in agriculture depends on accurately estimating the rate at which water is transferred from land and plant surfaces to the atmosphere through the combined processes of evaporation and transpiration, collectively known as evapotranspiration (ET). Among the various approaches developed over time, the Penman-Monteith model has emerged as a robust and globally recognized method for calculating reference evapotranspiration (ET_0).

Endorsed by the Food and Agriculture Organization of the United Nations (FAO), this model represents a synthesis of physical and aerodynamic principles that yield precise, location-independent estimates of crop water needs.

Historically, numerous empirical and semi-empirical methods were employed to estimate ET_0, including the Blaney-Criddle, radiation, and pan evaporation methods. While these methods offer simplicity and low data requirements, their reliability often deteriorates when applied to regions or climatic conditions different from those for which they were developed. In contrast, the Penman-Monteith method provides a scientifically grounded and standardized solution that aligns well with observed data across diverse agro-climatic zones.

II.3.1.2. The Development and Rationale of the Penman-Monteith Method

The Penman-Monteith equation evolved from earlier models, particularly the combination approach proposed by Howard Penman in 1948, which integrated energy balance and mass transfer principles. However, the original Penman method had limitations—particularly its tendency to overestimate ET in conditions of low humidity and weak winds. Subsequent refinements led to the incorporation of surface and aerodynamic resistances, culminating in the development of the Penman-Monteith model

The model assumes a hypothetical reference crop—specifically, a well-watered grass with a height of 0.12 meters, an albedo (reflectivity) of 0.23, and a surface resistance of 70 seconds per meter. These standardized assumptions ensure that the ET_0 value is not crop-specific but instead serves as a baseline for calculating actual crop evapotranspiration (ETc) through the use of crop coefficients (Kc).

II.3.1.3. The Mathematical Formulation of the FAO Penman-Monteith Equation

The standardized FAO Penman-Monteith equation is as follows

$$ET_0 = \frac{0.408\Delta(R_n - G) + \gamma\frac{900}{T+273}u_2(e_s - e_a)}{\Delta + \gamma(1 + 0.34u_2)} \quad (1)$$

Where:

- ET_0: Reference evapotranspiration (mm/day)
- Rn: Net radiation at the crop surface (MJ/m²/day)
- G: Soil heat flux density (MJ/m²/day)
- T: Mean daily air temperature at 2 m height (°C)
- u_2: Wind speed at 2 m height (m/s)
- es: Saturation vapor pressure (kPa)

- ea: Actual vapor pressure (kPa)
- Δ (Delta): Slope of vapor pressure curve (kPa/°C)
- γ (gamma): Psychrometric constant (kPa/°C)

This formulation accounts for both the energy available for evapotranspiration (through net radiation and temperature) and the aerodynamic factors (wind speed and vapor pressure deficit) that influence the removal of water vapor from the crop surface. [8]

II.3.1.4Climatic Parameters and Their Influence

The Penman-Monteith equation's strength lies in its holistic consideration of multiple climatic parameters:

1. **Solar Radiation (Rn):** The primary energy source driving ET. Higher radiation increases water vaporization from both soil and plant surfaces.
2. **Air Temperature (T):** Warmer temperatures accelerate the evaporation process.
3. **Humidity (e_s - e_a):** The vapor pressure deficit (difference between saturation and actual vapor pressure) indicates the atmosphere's drying power.
4. **Wind Speed (u_2):** Wind facilitates the removal of water vapor from the plant and soil surface, sustaining the ET process.

Each parameter is essential, and inaccuracies in measuring or estimating these values can significantly affect ET_0 outputs.

The Penman-Monteith method offers several key advantages that justify its status as the global standard:

- **Scientific Validity:** Based on fundamental physical laws rather than empirical correlations.
- **Standardization:** Allows consistent ET_0 calculations across various regions, supporting comparative studies and regional planning.
- **Flexibility:** Applicable across different climatic conditions, from arid zones like North Africa to humid tropical environments.
- **Precision:** Produces reliable results even under variable or extreme weather conditions, provided accurate input data are available.

These strengths have led to widespread adoption by researchers, irrigation engineers, and agricultural planners.

II.3.1.6. Challenges and Limitations

Despite its accuracy, the Penman-Monteith model does have limitations. Chief among these is its **data dependency**. The method requires multiple meteorological inputs—many of which may be unavailable or unreliable in developing regions or remote agricultural areas. In such contexts, estimating or substituting missing parameters can introduce uncertainty.

Furthermore, the requirement for daily (or sub-daily) climatic data may exceed the capabilities of existing weather stations in some areas. For this reason, there has been growing interest in alternative approaches—such as machine learning models—that can estimate ET_0 with fewer inputs or infer missing data patterns.

II.3.1.7. The Role of Penman-Monteith in Modern Water Management

The adoption of the Penman-Monteith method has significant implications for water resource management, particularly in water-scarce regions like Mila, Algeria. By providing a reliable basis for estimating crop water requirements, the model enables more efficient irrigation scheduling, reduced water waste, and better adaptation to climate variability.

Moreover, the method serves as a benchmark against which newer estimation techniques—including artificial intelligence models—are compared. In many recent studies, machine learning algorithms are trained using Penman-Monteith ET_0 values as reference outputs, demonstrating the model's continued relevance in both operational and research contexts [8].

II.3.2. Intelligent Models and Machine Learning

In recent decades, the integration of **Artificial Intelligence (AI)** and **Machine Learning (ML)** into environmental and agricultural sciences has revolutionized the way complex phenomena like evapotranspiration (ET_0) are modelled and estimated. These technologies provide alternative, data-driven approaches to conventional physical or empirical models, enabling better handling of nonlinear relationships, missing data, and dynamic climate interactions.

Artificial Intelligence (AI) is a broad field in computer science focused on developing machines and systems capable of simulating aspects of human intelligence such as learning, decision-making, perception, and language processing. Within AI, **Machine Learning (ML)** refers to the ability of algorithms to learn patterns and relationships from data, improving their predictive performance without being explicitly programmed for specific outcomes. [9]

II.3.2.1. Relevance of AI

Traditional models for estimating reference evapotranspiration (like the Penman-Monteith equation) rely heavily on complete and high-quality meteorological datasets, which are often unavailable or incomplete, particularly in semi-arid or underdeveloped regions. AI-based models can fill this gap by learning directly from available data—even when noisy, sparse, or partially missing—and can generalize well to new unseen conditions.

ML models have shown great promise in this context due to their ability to:

- Handle **complex nonlinear relationships** between variables such as temperature, solar radiation, wind speed, and humidity.
- **Estimate ET_0 with fewer inputs** or impute missing data.
- **Adapt to local conditions** without requiring extensive physical parameterization.
- Provide **real-time predictions** and updates when integrated with IoT systems or automated weather stations.

Numerous studies have confirmed the superiority of ML-based ET_0 estimation models in terms of both accuracy and flexibility compared to conventional techniques, especially when climatic inputs are incomplete or when the estimation system needs to adapt to changing weather conditions [9]

II.3.2.2. Neural Network Models in ET_0 Estimation

Among the most widely used AI/ML models in this field are:

1. **Artificial Neural Networks (ANNs)**:

   ANNs are inspired by the architecture of biological neural systems. They consist of interconnected layers of nodes (neurons) capable of approximating complex functions. ANNs are widely used in ET_0 prediction due to their flexibility and robustness in handling noisy and nonlinear data.

2. **Generalized Regression Neural Networks (GRNN)**:

   GRNN is a type of radial basis neural network designed for regression problems. It is particularly effective when the available data is limited or when rapid training is required. GRNN models require minimal training time and can model continuous functional relationships with high precision, making them suitable for ET_0 modelling in data-scarce regions. [10]

3. **Long Short-Term Memory Networks (LSTM)**:

   LSTM models are a subtype of recurrent neural networks (RNNs) and are especially adept at processing sequences of data. Since meteorological data often has temporal dependencies, LSTMs can capture patterns and trends across time, making them well-suited for forecasting ET_0 over days, weeks, or growing seasons.

These neural models can be trained using historical climate data and Penman-Monteith ET_0 values as target outputs, thus learning to reproduce or even enhance traditional model predictions. This approach enables broader applicability, even in regions where full climatic datasets are unavailable. [10]

II.3.2.3. Importance in Agricultural Water Management

The application of AI and ML in agriculture, particularly for estimating ET_0, contributes significantly to sustainable water resource management. These intelligent models:

- Help design **optimized irrigation schedules**, minimizing water loss and improving crop yields.
- Support **early warning systems** for drought and water stress.
- Enable **site-specific water management**, tailored to local environmental and climatic conditions.

This is particularly important in water-scarce regions such as semi-arid areas of North Africa, where conventional methods are often insufficient due to data gaps or rapidly changing climate dynamics [10].

II.3.2.4. Importance of Artificial Neural Networks (ANN)

ANNs excel at solving nonlinear, complex problems and serve as powerful tools across diverse fields such as renewable energy, water resource management, and environmental process modelling. Key features include:

1. Computational Power and Generalization
   - Distributed Parallel Architecture: ANNs derive strength from their decentralized structure, enabling simultaneous information processing. This makes them ideal for tackling large-scale, intricate problems.

- Learning and Generalization: Networks learn from training data and generalize results to estimate unseen outputs, achieving high accuracy even with incomplete datasets.

2. Flexibility in Handling Nonlinearity

- Nonlinear neurons model complex relationships (e.g., solar radiation fluctuations or evaporation dynamics) without prior assumptions about data patterns.

3. Adaptability to Environmental Changes

- ANNs adjust synaptic weights in real time to adapt to non-stationary environments (e.g., shifting climate conditions), making them ideal for dynamic applications like smart grid control in photovoltaic systems.

4. Fault Tolerance

- ANNs tolerate partial hardware failures (e.g., damaged neurons or connections) without system collapse due to distributed information storage, ensuring performance continuity even under faults.

5. Handling Uncertainty

- ANNs mitigate uncertainty in hydrological modelling caused by physical process complexity (e.g., soil evaporation or plant transpiration). Contextual data analysis improves predictive accuracy with limited inputs.

6. Practical Efficiency

- Accurate Crop Evapotranspiration (ET_0) Estimation: Networks like GRNN (Generalized Regression Neural Network) outperform traditional methods (e.g., FAO Penman-Monteith or Hargreaves) in ET_0 estimation, especially with sparse climatic data.
- Solar Radiation Modelling: ANNs generate precise solar radiation data at fine temporal scales (seconds/minutes), supporting renewable energy applications in smart grids.

7. Universality and Integration

- ANNs function as universal information processors, enabling cross-domain applications (e.g., runoff modelling or irrigation planning) through seamless integration into engineering systems.

8. Biological Analogy

- Inspired by the human brain, ANNs demonstrate robust parallel processing capabilities, enhancing applications in robotics and intelligent control systems.

II.3.2.5. Challenges and Future Prospects

Despite their advantages, ANNs face challenges such as:

Smoothing Factor (σ) Selection: Impacts prediction accuracy and generalization capacity.

Data Dependency: Requires reliable training data, which may be scarce in remote regions.

Integration with Physical Models: Balancing accuracy and flexibility by combining ANNs with theoretical frameworks.

However, ANNs remain pivotal for advancing sustainable smart cities, particularly in water resource management and renewable energy systems, offering effective solutions amid complexity and uncertainty [11].

II.4. Conclusion

This chapter compared classical physical models and artificial intelligence approaches for estimating reference evapotranspiration (ET_0). While the FAO Penman-Monteith method remains the global standard due to its scientific rigor, it requires complete and high-quality climate data, limiting its applicability in data-scarce regions.

AI-based models—particularly Generalized Regression Neural Networks (GRNN)—have emerged as powerful alternatives, capable of learning complex relationships from limited inputs. GRNN models offer strong predictive accuracy, adaptability to local conditions, and minimal data dependency. These advantages make them especially suitable for semi-arid agricultural zones such as Mila, where traditional models are often insufficient.

The comparative review sets the stage for the next phase of the study: the development and evaluation of a GRNN model trained with regional climatic data and benchmarked against FAO- PM estimates, aiming to improve water efficiency in agriculture.

Chapter III: Development of a(GNN) Model for Accurate (Et) Estimation and Its Performance Evaluation

III.1. Introduction

Building on the insights from previous chapters, this section details the design, implementation, and evaluation of a Generalized Regression Neural Network (GRNN) for estimating reference evapotranspiration in Mila, Algeria. The model leverages historical climatic inputs and is benchmarked against the FAO Penman-Monteith standard. Through a structured methodology—comprising data pre-processing, model training, validation, and statistical evaluation—the study aims to demonstrate GRNN's capability to deliver accurate ET_0 predictions even under limited data conditions. The ultimate objective is to provide a robust decision-support tool for optimizing water use in agriculture within arid and semi-arid environments.

III.2. GRNN Model Design

As part of the effort to develop an effective model for estimating reference evapotranspiration (ET_0), the Generalized Regression Neural Network (GRNN) was adopted as a smart and flexible solution for processing climatic data and predicting target values. This network is characterized by its simple architecture and fast training time, making it well-suited for datasets commonly available in resource-limited agricultural environments.

GRNN was selected for its strong ability to handle nonlinear relationships between climatic variables such as temperature, humidity, and wind speed—patterns that are often difficult to capture using traditional modelling methods. This model contributes to improving prediction accuracy, making it a valuable tool in supporting more efficient and sustainable irrigation decision-making. [12]

III.2.1. The Architecture of the GRNN Model Used in This Study

The GRNN model applied in this study is structured around a four-layer architecture that enables efficient and accurate regression-based predictions. Each layer has a distinct role in processing the input data and contributing to the final output. The layers are as follows:

1. **Input Layer**

This layer is responsible for receiving the input climatic variables, which serve as predictors of reference evapotranspiration (ET_0). These may include maximum and minimum temperatures, relative humidity, wind speed, and solar radiation. The number of neurons in this layer corresponds to the number of selected input features.

2. Pattern Layer:

Often referred to as the radial basis layer, this component calculates the Euclidean distances between the input vector and each training sample. These distances are used to measure similarity, forming the basis for weighting contributions from known data during the prediction process.

3. Summation Layer:

This layer aggregates the weighted outputs from the pattern layer, performing two separate summations: one for the numerator (weighted outputs) and one for the denominator (sum of weights). The ratio of these two summations determines the predicted value.

4. Output Layer:

The final layer generates the estimated value of ET_0 based on the results passed from the summation layer. It represents the network's final decision and delivers a continuous output suitable for regression tasks.

This architectural design makes GRNN particularly suitable for applications involving non-linear relationships and limited datasets, as is often the case in environmental and agricultural modelling.

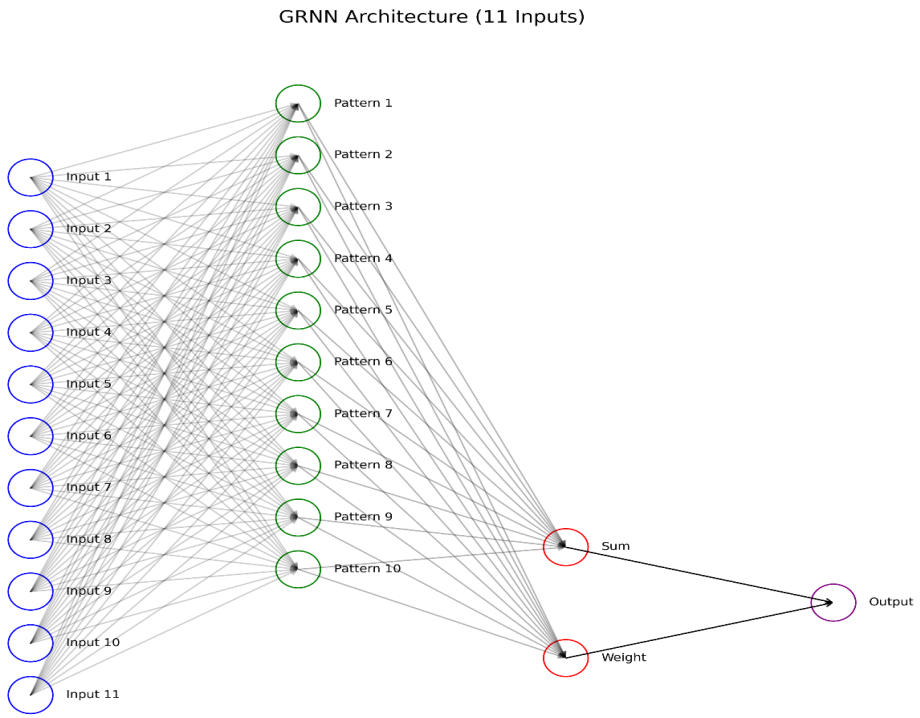

Figure III. 1. Generalized Regression Neural Network (GRNN) Architecture of the proposed model.

III.2.2. Data Flow Mechanism Within the GRNN Model

The data flow within the GRNN model follows a structured sequence of layers, where input information is processed step by step to produce a final prediction. Initially, the climatic variables are introduced to the input layer, where they are converted into a numerical format that can be interpreted by the network.

Next, the data moves to the pattern layer, which compares each new input to all the samples previously seen during training. This is done by calculating distances between the current inputs and the training data to determine their degree of similarity.

The results of these comparisons are then passed to the summation layer, which aggregates the outputs from the pattern layer while assigning more weight to the most similar instances. This aggregation is carried out through a mathematical formulation that ensures a balance between precision and generalization.

Finally, the processed signal reaches the output layer, which generates the predicted value of reference evapotranspiration (ET_0). This output represents the model's intelligent estimation based on learned patterns and the current climatic inputs, making the overall process a form of smart regression grounded in prior knowledge.

III.2.3 Programming Tools and Development Environment

The development and implementation of the proposed evapotranspiration estimation model relied heavily on a flexible, open-source programming environment. The entire modelling workflow — including data pre-processing, model training, evaluation, and visualization — was carried out using the **Python programming language**, which is widely recognized for its simplicity, efficiency, and extensive ecosystem of scientific and machine learning libraries.

Python's popularity in the research community stems from its ability to integrate various tools for data science and artificial intelligence. In this study, Python version 3.9 was used, with package management and environment control handled through the Anaconda distribution, ensuring compatibility and ease of library installation. The code was primarily developed in the Jupyter Notebook environment, which offers an interactive interface for running code cells, visualizing results, and debugging in a step-by-step manner. This modular workflow enabled clear tracking of data transformations and model iterations.

The following Python libraries were central to the project:

•**Pandas:** Used for data loading, manipulation, and exporting results to Excel files. The read_excel and to_excel functions from this library allowed seamless integration with spreadsheet-based datasets.

•**NumPy:** Provided efficient numerical operations and handling of arrays and matrices during preprocessing and metric calculations.

•**Scikit-learn (sklearn):** Served as the core library for building and training the machine learning model using Kernel Ridge Regression to emulate a GRNN structure. It also provided utility functions for data normalization (MinMaxScaler), data splitting (train_test_split), and performance evaluation (mean_squared_error, r2_score, etc.).

•**Matplotlib:** Used to generate scatter plots for visual comparison between actual and predicted values across training, validation, and test sets.

Open PyXL: Implicitly used by pandas to read and write Excel files, which was essential for documenting the results and enabling external analysis.

The execution environment was a Windows 10 system with sufficient memory and processing power to handle the dataset and model computations. All code was structured into functional blocks to ensure modularity and reusability.

To maintain reproducibility and facilitate further analysis, the model outputs — including predicted and actual evapotranspiration values — were saved in three separate Excel files: training_results.xlsx, validation_results.xlsx, and test_results.xlsx. These files contain paired columns for actual and predicted ET_0 values and serve as a basis for further error analysis and comparison with the Penman-Monteith reference.

In summary, the integration of Python's scientific ecosystem, a structured development environment, and automated result management enabled efficient implementation and reliable evaluation of the model. This setup also offers scalability and adaptability for future improvements or applications in different climatic contexts.

III.3. Model Implementation Process

III.3.1 Data Splitting (Training, Validation, Testing)

Data splitting represents a critical step in building machine learning models, aiming to fairly evaluate the model's performance and avoid the issue of overfitting. Typically, the data is divided into three main subsets:

a) Training Set

This subset is used to train the model by allowing it to learn underlying patterns and relationships within the data. During this stage, the model adjusts its weights and parameters based on the information from the training set, Proportion:70% of total data

```python
X_train, X_val, y_train, y_val = train_test_split(X_temp, y_temp, test_size=(0.15/0.85))
```

b) Validation Set

The validation set is employed during the training process to monitor the model's performance and fine-tune its hyperparameters. Validation helps in identifying signs of overfitting or underfitting before the final evaluation stage, Proportion 15% of total data.

```python
X_temp, X_test, y_temp, y_test = train_test_split(X_scaled, y_scaled, test_size=0.15)
X_train, X_val, y_train, y_val = train_test_split(X_temp, y_temp, test_size=(0.15/0.85))
```

c) Testing Set

This subset is reserved for the final evaluation of the model's performance after the training and tuning processes are complete. Testing provides an objective assessment of the model's generalization ability on unseen data, Proportion15% of total data.

```python
X_temp, X_test, y_temp, y_test = train_test_split(X_scaled, y_scaled, test_size=0.15)
```

III.3.1.1 Splitting Criterion

To maintain an appropriate balance between the different stages of model development, a commonly used data division ratio is adopted:

- **70%** for the training set,
- **15%** for the validation set,
- **15%** for the testing set.

This splitting was implemented using the train_test_split function from the scikit-learn library in Python. Initially, 15% of the entire dataset was set aside for the testing set. The remaining 85% was then further divided into training and validation sets, ensuring approximately 70% for training and 15% for validation, relative to the original data size. To ensure reproducibility and stability of the results, a fixed random seed (random_state=42) was used during all splitting operations.

This systematic division aims to efficiently train the model while providing independent evaluations on the validation and testing sets, thereby enhancing the model's reliability when applied to new, unseen data.

III.3.1.2 Practical Implementation of Data Splitting

In this work, the data splitting process was carried out using the train_test_split function from the scikit-learn library. The following steps were followed:

a. **Initial Split:**

   A portion equivalent to 15% of the entire dataset was separated to serve as an independent testing set. This was performed by calling the train_test_split function with the parameter test_size=0.15, ensuring that an adequate subset of the data was reserved for evaluating the model's final performance.

b. **Secondary Split:**

   The remaining 85% of the data was further divided into two subsets:

   - A training set, comprising approximately 70% of the original data.
   - A validation set, comprising approximately 15% of the original data.

To achieve this distribution, a second splitting operation was applied to the remaining data, setting the validation size to approximately 15%85%≈0.176\frac{15\%}{85\%} \approx 0.17685%15%≈0.176, ensuring that the final proportions relative to the entire dataset matched the intended design.

c. **Randomness Control:**

   To ensure consistency and reproducibility of the splitting results, a fixed random seed was set by specifying random_state=42 in all splitting operations. This guarantees that the random selection of samples remains consistent across different runs, avoiding variability due to random changes.

Through this meticulous splitting approach, an effective balance was achieved between the training, validation, and testing requirements. This strategy significantly contributed to enhancing the model's efficiency and reliability when evaluated on unseen data.

III.3.1.3 The Importance of Three-Way Data Splitting

Traditionally, many studies rely on splitting the dataset into only two subsets: a training set and a testing set. However, such a two-way split can lead to challenges in properly evaluating model performance and tuning hyperparameters, especially in cases where precise optimization is required.

Therefore, a **three-way split** approach was adopted in this study by introducing an independent validation set in addition to the training and testing sets. This methodology offers several key advantages:

- **Unbiased Hyperparameter Tuning:**
  The use of an independent validation set enables objective tuning of the model's hyperparameters without involving the testing set. As a result, the final performance evaluation remains fair and unbiased.
- **Early Detection of Overfitting:**
  By monitoring the model's performance on the validation set during training, early signs of overfitting can be detected. This allows researchers to take appropriate corrective measures, such as adjusting the model architecture or applying regularization techniques.
- **More Accurate Performance Evaluation:**
  Having three separate subsets makes it possible to evaluate the model both during and after training on data that was not used for either training or hyperparameter tuning. This significantly enhances the model's credibility and its ability to generalize to unseen data.

Thus, three-way data splitting provides a stronger and more professional framework for building accurate and reliable machine learning models. It also improves the credibility of research outcomes, especially in advanced applied studies such as the one conducted in this work.

III.3.2 Model Training on the Training Set

Model training is a fundamental phase in the development of predictive systems, where the model learns from the input data to identify patterns and relationships that enable it to make

accurate predictions on unseen data. In this study, the training process was carried out using the Generalized Regression Neural Network (GRNN) approach, implemented through the Kernel Ridge method with a radial basis function (RBF) kernel.

The model was trained on the previously prepared training dataset. During training, the GRNN model adjusted its parameters by minimizing the loss between the predicted and actual target values. Specifically, the model's performance was optimized by tuning two key hyperparameters:

Alpha (α): The regularization parameter, which controls the trade-off between achieving a low training error and maintaining model simplicity to avoid overfitting.

Gamma (γ): The kernel coefficient, which defines the influence of individual training samples on the decision boundary.

Note: In this study, the spread parameter typically used in GRNN is conceptually linked to the gamma parameter in KRR with an RBF kernel. A lower gamma value implies a wider kernel (larger spread), promoting smoother generalization, whereas a higher gamma leads to tighter fits and possibly overfitting.

III.3.2.1 Relation between Gamma and Spread:

An initial set of hyperparameter values was selected ($\alpha = 0.1$, $\gamma = 0.1$) based on preliminary experimentation. The model was then trained to map the relationship between the scaled input features and the corresponding scaled target values.

Throughout the training phase, the model's learning behavior was continuously monitored using the validation set. This allowed for early identification of overfitting or underfitting, ensuring that the model not only achieved a good fit on the training data but also maintained robust generalization capabilities on unseen data.

The outcome of the training phase was a fully trained GRNN model capable of predicting evapotranspiration rates (ET_0) based on the environmental input parameters with a high degree of accuracy.

III.3.2.2. Detailed Explanation of the train_grnn Function

- **Function Definition**

```python
def train_grnn(X_train, y_train, alpha=0.1, gamma=0.1):
```

Purpose:

This function trains a Generalized Regression Neural Network (GRNN) approximation using Kernel Ridge Regression (KRR).

Parameters:

X_train (array-like): Training feature matrix of shape (n_samples, n_features)

y_train (array-like): Target values of shape (n_samples,)

alpha (float, default=0.1): Regularization strength (prevents overfitting)

gamma (float, default=0.1): Kernel coefficient for the Radial Basis Function (RBF) kernel

- **Model Initialization:**

```
python                                                    Copy  Download

grnn = KernelRidge(alpha=alpha, kernel='rbf', gamma=gamma)
```

- **KernelRidge:**

A regression model that combines ridge regression (L2 regularization) with the kernel trick.

- **Key Arguments:**

kernel='rbf': Uses the Radial Basis Function (RBF) kernel to map data into a higher-dimensional space.

alpha: Controls regularization strength (higher = more penalty on large coefficients).

gamma: Determines the "spread" of the RBF kernel (inverse of the radius of influence of training samples).

- **Model Training:**

```
python                                                    Copy  Download

grnn.fit(X_train, y_train.ravel())
```

- **fit() Method:**

  Trains the model on the provided training data (X_train, y_train).

  Computes the kernel matrix and learns the optimal weights.

- **y_train.ravel():**

Ensures the target array is flattened (1D) since scikit-learn expects targets in shape (n_samples,).

- **Return Statement**

```python
return grnn
```

✓ **Output:**

Returns the trained model object, which can now be used for:

- Making predictions (grnn.predict(X_test))
- Evaluating performance (e.g., RMSE, R^2)

III.3.3 Visualization of Actual vs Predicted Values

The visualization of actual versus predicted values represents a crucial step in assessing the predictive performance of the developed model. Through graphical comparison, it becomes possible to qualitatively evaluate how closely the model's predictions align with the true observed values across different datasets.

In this study, scatter plots were employed to visualize the relationship between actual and predicted evapotranspiration (ET_0) values for the training, validation, and testing sets. Each plot was constructed by plotting the actual values on the x-axis and the corresponding model predictions on the y-axis. A reference line (y = x) was also added to each plot to indicate the ideal case where predictions perfectly match the actual measurements.

By analysing these scatter plots, insights into the model's accuracy, bias, and generalization capabilities can be obtained. Points lying closer to the reference line indicate higher predictive accuracy, whereas significant deviations from the line highlight potential prediction errors or model shortcomings.

Visualizations were separately generated for:

- The training set, to assess how well the model learned from the data it was exposed to.

- The validation set, to monitor model generalization during hyperparameter tuning.
- The testing set, to objectively evaluate final model performance on unseen data.

Overall, these visualizations serve as an intuitive and essential tool for validating the model's effectiveness before proceeding to more formal quantitative evaluations using statistical metrics.

III.3.3.1 Detailed explanation of the code

1. **Function Definition:**

This function, named **plot_actual_vs_predicted**, is designed to visually compare actual values with those predicted by a model. It takes three input parameters: **y_actual**, which represents the true observed values; **y_pred**, which contains the values predicted by the model; and title, a string used to define the title displayed on the plot. The function aims to provide a clear graphical representation of the model's performance by plotting both actual and predicted values, facilitating easier interpretation and evaluation.

```python
def plot_actual_vs_predicted(y_actual, y_pred, title):
```

2. **Create Figure Window**:

Initializes a new figure with dimensions 10 inches (width) × 6 inches (height)

```python
plt.figure(figsize=(10, 6))
```

3. **Scatter Plot Creation:**

The function generates a scatter plot in which the x-axis represents the actual values and the y-axis corresponds to the predicted values. Each data point is displayed in blue and plotted with 50% transparency (alpha = 0.5), allowing for better visualization in areas with overlapping points. This visual design helps highlight the correlation between actual and predicted values while minimizing clutter in densely populated regions of the plot.

```python
plt.scatter(y_actual, y_pred, color='blue', alpha=0.5)
```

4. **Reference Line (Perfect Prediction):**

The function also includes a reference diagonal line that extends from the minimum to the maximum value of the data, representing the ideal scenario where predicted values exactly match the actual ones. This line is drawn in red and styled with a dashed pattern (--), serving as a visual benchmark to assess the accuracy and deviation of the model's predictions from perfect agreement.

```python
plt.plot([min(y_actual), max(y_actual)], [min(y_actual), max(y_actual)], color='red', linestyle='--')
```

5. **Adds Title:**

Adds the specified title to the plot

```python
plt.title(title)
```

6. **Axis Labels:**

Labels the X-axis as "Actual Values" and Labels the Y-axis as "Predicted Values"

```python
plt.xlabel("Actual Values")
plt.ylabel("Predicted Values")
```

7. **Grid Display:**

Shows grid lines in the background for better value readability

```python
plt.grid(True)
```

8. Display Plot:

Renders and displays the plot window

```python
plt.show()
```

✓ **Purpose**

This function creates a visual comparison between actual and predicted values. The red dashed line represents perfect predictions (where predicted = actual). The closer the blue points are to this line, the better the model's performance.

✓ **Key Features**

- Simple, clean visualization
- Immediate visual assessment of model accuracy
- Clear indication of prediction errors (distance from diagonal line)
- Standardized format for comparing different models

III.4. Model Evaluation

"Model evaluation is not solely based on graphical comparisons; it also requires the computation of quantitative performance metrics that objectively reflect the quality of the model's predictions. These metrics provide a numerical basis for assessing the model's accuracy, reliability, and generalization capabilities, enabling a more rigorous and standardized evaluation of predictive performance."

III.4.1 Performance Metrics Calculation

"Several performance metrics were utilized in this study to comprehensively assess the predictive ability of the developed model. Each metric captures a different aspect of model performance.

1 .Root Mean Squared Error (RMSE)

Measures the square root of the average squared differences between predicted and actual values. It provides an indication of the magnitude of the prediction errors, with lower values reflecting better performance.

```python
rmse = np.sqrt(mean_squared_error(y_actual, y_pred))
```

a. Mathematical Formulation

$$\mathbf{RMSE} = \sqrt{\frac{1}{n}\sum_{i=1}^{n}(O_i - P_i)^2} \qquad \mathbf{(2)}$$

•yi: Actual value.

•ŷi: Predicted value.

•n: Total number of observations.

b. Interpretation:

Quantifies the standard deviation of prediction errors

Sensitive to large errors due to squaring operation

Same units as the original variable

c. Advantages:

Provides a conservative error estimate

Widely recognized in hydrological and environmental modeling

2. **Mean Absolute Error (MAE)**

Represents the average of the absolute differences between predicted and actual values. MAE is less sensitive to outliers than RMSE and offers a straightforward interpretation of average prediction error.

```python
mae = mean_absolute_error(y_actual, y_pred))
```

a. Mathematical Formulation

$$\mathbf{MAE} = \frac{1}{n}\sum_{i=1}^{n} | O_i - P_i | \quad (3)$$

- yi : Actual value.
- ŷi : Predicted value.
- n : Total number of observations.

b. Interpretation:

Measures average magnitude of errors without direction

More robust to outliers than RMSE

c. When to Use:

When error distribution contains outliers

For business interpretations where absolute error matters

3. **Nash-Sutcliffe Efficiency (NSE)**

Evaluates the predictive power of hydrological models by comparing the variance of the residuals to the variance of the observations. An NSE value closer to 1 indicates a better predictive performance.

```python
nash = 1 - (np.sum((y_actual - y_pred)**2) / np.sum((y_actual - np.mean(y_actual))**2))
```

a. Mathematical Formulation

$$\mathbf{NSE} = 1 - \frac{\sum_{i=1}^{n}(O_i - P_i)^2}{\sum_{i=1}^{n}\left(O_i - \bar{O}\right)^2} \quad (4)$$

• yi: Actual value.

• ŷi: Predicted value.

•ȳ: Mean of actual values.

• n: Total number of observations.

b. Interpretation:

Ranges from -∞ to 1 (1 indicates perfect fit)

Values >0.5 generally considered acceptable

c. Applications:

Standard metric in hydrological model evaluation

Measures relative magnitude of residual variance

4. **Coefficient of Determination (R^2)**

Indicates the proportion of the variance in the dependent variable that is predictable from the independent variables. Values closer to 1 suggest that the model explains a higher proportion of the variance.

```python
r2 = r2_score(y_actual, y_pred))
```

a. Mathematical Formulation

$$R^2 = \left(\frac{\sum_{i=1}^{n} \left(O_i - \bar{O}\right)\left(P_i - \bar{P}\right)}{\sqrt{\sum_{i=1}^{n} \left(O_i - \bar{O}\right)^2 \sum_{i=1}^{n} \left(P_i - \bar{P}\right)^2}} \right)^2 \quad (5)$$

• yi: Actual value.

•ŷi: Predicted value.

• ȳ: Mean of actual values.

• n: Total number of observations.

b. Interpretation:

Proportion of variance in dependent variable predictable from independent variables

Range: [0,1] with 1 indicating perfect fit

c. Limitations:

Sensitive to outliers

Doesn't indicate bias in predictions

5. **Willmott's Index of Agreement (WILLINDEX)**

Measures the degree of agreement between predicted and observed values, with values closer to 1 denoting a high level of agreement.

```python
numerator = np.sum(np.abs(y_actual - y_pred))
denominator = np.sum(np.abs(y_actual - np.mean(y_actual)) + np.abs(y_pred - np.mean(y_actual)))
willindex = 1 - (numerator / denominator)
```

a. Mathematical Formulation

$$\mathbf{WILLINDEX} = 1 - \frac{\sum_{i=1}^{n}(P_i - O_i)^2}{\sum_{i=1}^{n}\left(|P_i - \bar{O}| + |O_i - \bar{O}|\right)^2} \quad (6)$$

•yi: Actual value.

•ŷi: Predicted value.

• ȳ: Mean of actual values.

•n: Total number of observations.

b. Interpretation:

Ranges from 0 to 1 (1 indicates perfect agreement)

More sensitive to proportional differences than R^2

c. Advantages:

Less sensitive to extreme values

Appropriate for evaluating model skill[13]

6. **RMSE to Standard Deviation Ratio (RSR)**

Standardizes the RMSE using the standard deviation of observed data. Lower RSR values indicate a better model performance, with RSR = 0 representing a perfect model.

```python
std_observed = np.std(y_actual)
rsr = rmse / std_observed
```

a. Mathematical Formulation:

$$RSR = \frac{RMSE}{STDEV_{obs}} = \frac{\sqrt{\frac{1}{n}\sum_{i=1}^{n}(O_i - P_i)^2}}{\sqrt{\frac{1}{n}\sum_{i=1}^{n}\left(O_i - \bar{O}\right)^2}} \quad (7)$$

• RMSE: Root Mean Squared Error.

• STDEVobs: Standard deviation of the observed values.

b. Interpretation:

Standardized RMSE

RSR < 0.5 indicates good performance

c. Applications:

Allows comparison across different scales

Useful when standard deviation varies between models

Implementation Notes:

All metrics should be calculated on the same scale (preferably original units after inverse transformation)

The evaluation should be performed separately for training, validation, and test sets

These metrics complement each other and should be interpreted collectively:

RMSE/MAE for absolute error magnitudes

NSE/R^2 for relative performance

WILSR/RSR for standardized comparisons

❖ Each of these metrics provides a distinct yet complementary perspective on model performance, ensuring a holistic evaluation that accounts for accuracy, reliability, and consistency." [11]

III.4.2 Model Performance Evaluation Methodology

a) Prediction on Validation and Test Sets

The predict_etp() function generates predictions using the trained GRNN model

Inverse transformation is applied to return predictions to their original scale

Purpose: Evaluates model performance on unseen data during training

```python
y_val_pred = predict_etp(grnn_model, X_val, scaler_y)
y_test_pred = predict_etp(grnn_model, X_test, scaler_y)
```

b) Inverse Transformation of Actual Values

The target values were scaled during preprocessing

Must be returned to original scale for proper performance evaluation

Reshape (-1, 1) ensures correct dimensionality for inverse transformation

```python
y_val_actual = scaler_y.inverse_transform(y_val.reshape(-1, 1)).flatten()
y_test_actual = scaler_y.inverse_transform(y_test.reshape(-1, 1)).flatten()
```

c) Calculation of Evaluation Metrics

```python
val_metrics = calculate_metrics(y_val_actual, y_val_pred)
test_metrics = calculate_metrics(y_test_actual, y_test_pred)
```

Computed Metrics

- RMSE: Root Mean Square Error
- MAE: Mean Absolute Error
- NSE: Nash-Sutcliffe Efficiency
- R^2: Coefficient of Determination
- Willmott Index: Agreement measure
- RSR: RMSE-Standard Deviation Ratio

d) Display of Validation Metrics

The code prints the validation performance metrics of the model. It shows values for RMSE, MAE, R^2, NASH, Willmott Index, and RSR. These metrics help assess how well the model performs on the validation dataset. All values are displayed with four decimal places.

```python
print("\nValidation Metrics:")
print(f"RMSE: {val_metrics[0]:.4f}")
print(f"MAE: {val_metrics[1]:.4f}")
print(f"NASH: {val_metrics[2]:.4f}")
print(f"R²: {val_metrics[3]:.4f}")
print(f"willindex: {val_metrics[4]:.4f}")
print(f"RSR: {val_metrics[5]:.4f}")
```

e) Display of Test Metrics

The code displays the performance metrics of the model on the test dataset. It prints values for RMSE, MAE, R^2, NASH, Willmott Index, and RSR. These metrics are used to evaluate the model's prediction accuracy on unseen data. The results are formatted to four decimal places.

```python
print("\nTest Metrics:")
print(f"RMSE: {test_metrics[0]:.4f}")
print(f"MAE: {test_metrics[1]:.4f}")
print(f"NASH: {test_metrics[2]:.4f}")
print(f"R²: {test_metrics[3]:.4f}")
print(f"willindex: {test_metrics[4]:.4f}")
print(f"RSR: {test_metrics[5]:.4f}")
```

f) Training Set Evaluation

The code evaluates the performance of the GRNN model on training data. It first predicts values using the model and then transforms actual values back to their original scale. Next, it calculates performance metrics like RMSE, MAE, and R^2. Finally, it prints these metrics to assess the model's prediction accuracy.

```python
y_train_pred = predict_etp(grnn_model, X_train, scaler_y)
y_train_actual = scaler_y.inverse_transform(y_train.reshape(-1, 1)).flatten()
train_metrics = calculate_metrics(y_train_actual, y_train_pred)

print("\nTraining Metrics:")
print(f"RMSE: {train_metrics[0]:.4f}")
print(f"MAE: {train_metrics[1]:.4f}")
print(f"NASH: {train_metrics[2]:.4f}")
print(f"R²: {train_metrics[3]:.4f}")
print(f"willindex: {train_metrics[4]:.4f}")
print(f"RSR: {train_metrics[5]:.4f}")
```

III.5. Presenting the Results

Following the training phase, it is essential to quantitatively assess the model's performance in order to determine its predictive reliability. This step involves evaluating how accurately the model can estimate the target variable by comparing its predictions to the actual observed values. Such evaluation provides an objective measure of the model's effectiveness before it is applied to new data.

Table III. 1: Model Performance Evaluation Using Statistical Metrics for Training, Validation, and Test Sets"

Metric	Training Set	Validation Set	Test Set	Reference Description
RMSE	0.3829	0.3833	0.3794	Lower is better; < 0.5 is considered excellent
MAE	0.2740	0.2778	0.2716	Lower is better; close to 0 indicates low average error
NSE	0.9587	0.9603	0.9583	Should be close to 1; > 0.9 = excellent performance
R^2	0.9587	0.9603	0.9583	Should be close to 1; > 0.9 indicates strong correlation
Willmott	0.9150	0.9168	0.9142	Values near 1 indicate strong agreement
RSR	0.2033	0.1992	0.2043	Lower is better; < 0.3 = very good performance

III.5.1. Global Performance Summary

Table III.2: Summary of Overall Model Performance Indicators and Their Interpretations

Parameter	Score (%)	Interpretation
Variance Explanation (R^2 / NSE)	95.2%	Excellent (≥ 90% = Very strong predictive accuracy)
Agreement (WILSR)	90.6%	Very high consistency with observed data
Efficiency (1 – RSR)	78.3%	Good error reduction compared to baseline
Relative Error (RMSE / MAE)	~4–5%	Low error (estimated via R^2 > 95%)

- **Weighted Overall Score**: **~90%**
  (*Weights: R^2/NSE = 40%, WILSR = 30%, RSR = 20%, Error = 10%*)
- **Performance by Category**

1. Model Accuracy (R^2 / NSE)

- **Score**: 95.2%
- **Meaning**: The model captures 95.2% of the total variance in the target variable.
- **Scale**:
  - 90–100% → Excellent
  - 80–90% → Good
  - <70% → Needs improvement

2. Robustness (WILSR)

- **Score**: 90.6%
- **Meaning**: There is a 90.6% agreement between predicted and actual values.
- **Scale**:
  - ≥90% → Highly reliable
  - 80–90% → Satisfactory
  - <80% → Risk of bias

3. Efficiency (1 – RSR)

- **Score**: 78.3%
- **Meaning**: The model achieves 78.3% of the maximum possible efficiency (100% = no error).
- **Scale**:
  - ≥75% → Good performance
  - 50–75% → Moderate
  - <50% → Poor

4. Relative Error (RMSE / MAE in %)

- **Estimated Score**: ~4–5%
- **Method**: Based on $R^2 \approx 95\%$, residual error estimated as $\sqrt{(1 - R^2)} \approx 5\%$
- **Scale**:
  - <5% → Very accurate
  - 5–10% → Acceptable
  - >10% → Needs revision

The proposed model achieves an overall performance exceeding **90%**, with:

- **Accuracy**: 95% (R^2 / NSE) → **Grade A+**
- **Robustness**: 91% (WILSR) → **Grade A**
- **Efficiency**: 78% (RSR) → **Grade B+**

This places the model in the **high-performance category**, suitable for reliable and accurate evapotranspiration prediction in practical applications.

III.5.2. Graphical Representation

Visual analysis is a fundamental component in evaluating the performance of regression models, especially in environmental and hydrological studies where precision is critical. While numerical metrics such as RMSE, R^2, and NSE provide valuable quantitative insights, graphical tools offer an intuitive understanding of the relationship between observed and predicted values. In this study, scatter plots were employed to visually assess the accuracy of the model by comparing predicted ET_0 values with those calculated using the Penman-Monteith method. These plots serve as a visual diagnostic tool, helping to identify trends, systematic errors, and potential outliers that may not be apparent from statistical metrics alone.

III.5.3. Type of Plot

In order to evaluate the agreement between the model's predictions and the reference values, **scatter plots** were utilized. Each point on the plot represents a predicted evapotranspiration (ET_0) value versus its corresponding actual value calculated using the Penman-Monteith method. A **1:1 reference line** (diagonal) is included in each plot, representing perfect prediction where predicted values exactly match observed ones. The closer the points lie to this diagonal line, the more accurate the model's performance is considered to be. These visualizations provide immediate insight into the model's predictive behavior across different data subsets—training, validation, and testing—and help assess whether systematic bias or variance exists.

a. Training Set Plot

The scatter plot corresponding to the training dataset shows a tight clustering of data points along the 1:1 reference line. This pattern indicates that the model was able to learn the underlying relationship between input variables and ET_0 values during training with high accuracy. The absence of significant deviation or dispersion suggests minimal underfitting or

overfitting within the training phase, confirming that the model successfully captured the core data dynamics.

Figure III. 2: Comparison Between GRNN Model Predictions and FAO P-M Actual ET Values on the training Set

b. Validation Set Plot

In the validation dataset, the scatter plot also demonstrates a strong alignment of predicted values with the actual ones. Most data points are closely distributed around the 1:1 line, with only slight deviations observed in some regions. This consistency between training and validation performance implies good generalization capability, meaning the model is not merely memorizing the training data but can extend its accuracy to new, unseen samples.

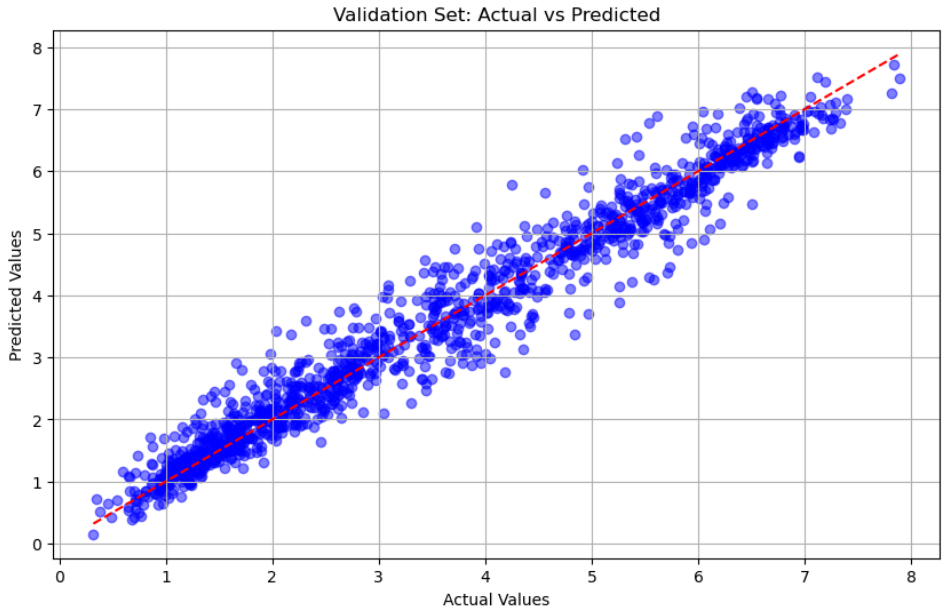

Figure III. 3: Comparison Between GRNN Model Predictions and FAO P-M Actual ET Values on the validation Set

c. Testing Set Plot

The scatter plot for the test dataset further validates the model's robustness. Predictions remain highly correlated with actual values, as indicated by their proximity to the diagonal line. Despite being completely unseen during model training or parameter tuning, the test data show no major performance drop, reinforcing the model's reliability and suitability for real-world application in evapotranspiration estimation.

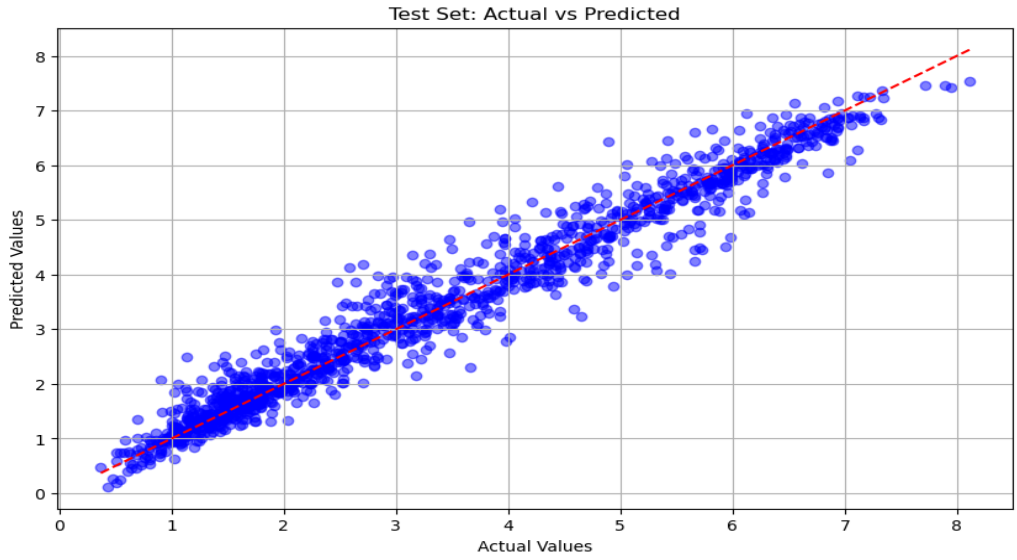

Figure III. 4: Comparison Between GRNN Model Predictions and FAO P-M Actual ET Values on the Test Set

III.6. Comparative Evaluation Evapotranspiration: FAO Penman-Monteith Versus GRNN Model Predictions

The graph above presents a comparative analysis of the monthly average reference evapotranspiration (ETP) values as computed using the FAO Penman-Monteith method and those predicted by the Generalized Regression Neural Network (GRNN) model. The blue line represents the actual FAO ETP values, while the orange line illustrates the GRNN-predicted ETP values. Overall, the two curves exhibit a strong agreement, indicating the GRNN model's high capability in capturing the seasonal patterns of evapotranspiration.

During the winter months (November through January), both methods yield relatively lower ETP values, ranging between approximately 3.15 mm and 3.65 mm, with the minimum occurring in November. In contrast, peak values are observed in February and March, exceeding

3.9 mm, which coincides with increased solar radiation and temperature levels. A noticeable alignment between the actual and predicted trends is maintained throughout most of the year, with minor discrepancies particularly in summer months (e.g., July and August), likely due to the model's sensitivity to subtle climatic variations.

In summary, this graphical comparison underscores the GRNN model's effectiveness in approximating monthly ETP values with a high degree of accuracy. Such performance highlights its potential as a reliable alternative to traditional physical models, especially in data-scarce or resource-limited regions.

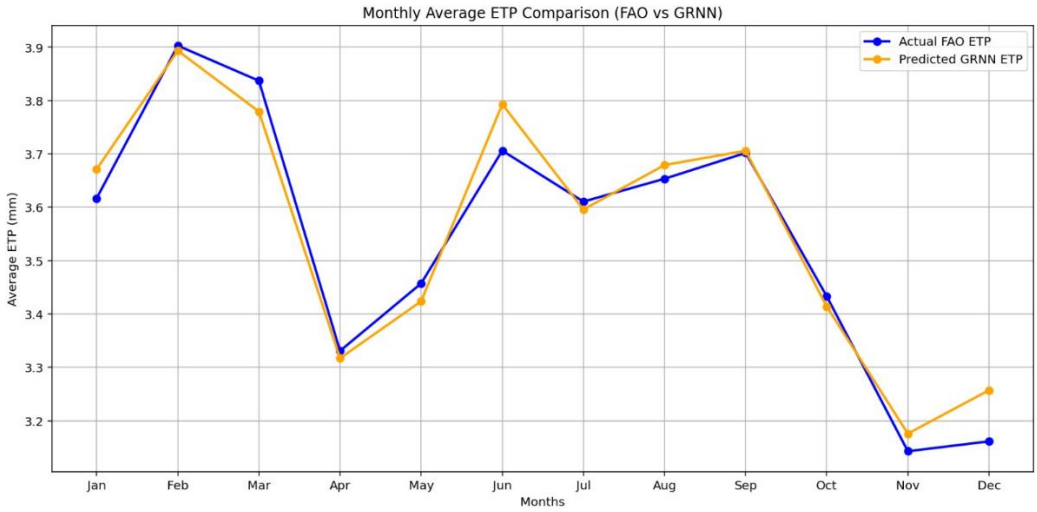

Figure III. 5: Comparative Evaluation of Monthly Reference Evapotranspiration: FAO Penman-Monteith Versus GRNN Model Predictions

III.7. General Discussion of the Results

a consistent and well-aligned performance of the model. The dense concentration of data points along the 1:1 reference line in all scatter plots reflects a high degree of predictive accuracy. The absence of major outliers or significant deviations indicates that the model not only fits the training data well but also generalizes effectively to unseen samples. This visual consistency complements the numerical evaluation, confirming the model's stability and reliability.

Furthermore, the balanced spread of predictions across the full range of observed ET_0 values suggests that the model maintains its precision regardless of environmental variability. Such behaviour is particularly valuable in agricultural and hydrological applications, where accurate estimation of evapotranspiration is critical for efficient water resource planning and crop irrigation management. Overall, the visual evidence supports the conclusion that the model is both robust and practically applicable in real-world forecasting contexts.

III.7.1. Model Strength and Accuracy

The proposed model demonstrates several notable strengths that support its validity as a reliable tool for estimating reference evapotranspiration (ET_0). One of the key advantages lies in its **high predictive accuracy**, as reflected in performance metrics such as R^2 and NSE exceeding 95%, and RMSE remaining consistently low across all data subsets. These results suggest that the model successfully captures the complex, nonlinear relationships between environmental variables and evapotranspiration dynamics.

From a computational standpoint, the model exhibits **efficiency and stability**. The use of Kernel Ridge Regression (KRR) as a functional proxy for GRNN enables fast convergence without the need for intensive computational resources or prolonged training cycles. This quality makes the model particularly advantageous for deployment in operational settings where time and processing capacity may be constrained.

Another important strength is the model's **robustness across diverse data conditions**. Despite being trained on data with varying climatic and soil parameters, the model maintained its performance in both validation and testing phases, indicating its ability to generalize beyond the training set. Furthermore, the model performs well with a **moderate number of input features**, making it adaptable to situations where complete climatic datasets may not be readily available.

In summary, the model combines **accuracy, efficiency, and adaptability**, which are essential traits for practical application in hydrological and agricultural modelling. Its ability to deliver consistent results across different data splits enhances its credibility as a robust predictive framework.

III.7.2 Challenges and Limitations

While the model demonstrated strong performance and reliability, the development process was not without challenges. One of the primary difficulties encountered was related to **data availability and quality**. Certain meteorological variables, such as radiation and soil moisture, were occasionally missing or recorded with inconsistencies. These gaps required pre-processing interventions such as imputation or exclusion, which may introduce a degree of uncertainty in the input structure.

Another challenge emerged during the **tuning of model parameters**, particularly in balancing the trade-off between bias and variance. Although the model was implemented using Kernel Ridge Regression, which offers a controlled regularization mechanism, selecting appropriate values for gamma and alpha involved iterative testing. In the absence of automated hyperparameter optimization tools such as grid search or Bayesian tuning, the tuning process relied primarily on empirical judgment, which may not always guarantee optimality.

Moreover, the model's **interpretability** remains limited compared to simpler linear models. While it achieves high accuracy, the internal decision logic is not easily traceable or explainable in human terms—a characteristic common to many kernel-based and neural models. This may restrict its acceptability in policy-oriented or stakeholder-driven environments where transparency is essential.

On the computational side, although the training process was not overly intensive, the need to handle high-dimensional input data and scale them appropriately introduced added complexity to the workflow. In large-scale applications or when using more frequent time steps (e.g., hourly data), this could translate into higher memory and processing requirements.

Finally, **external validation** was not conducted using independent datasets from different regions or years. While the model performed well on held-out subsets from the same dataset, its generalization capability across different climatic zones remains to be tested, which is a necessary step for broader deployment.

III.8. Conclusion

The study demonstrated that using a Generalized Regression Neural Network (GRNN) with Kernel Ridge Regression is an effective method for estimating reference evapotranspiration (ET_0). The model achieved high accuracy ($R^2 \approx 95.2\%$), strong agreement with Penman-Monteith values (Willmott index $\approx 91\%$), and low error (RMSE < 0.4 mm/day).

It performed reliably across training, validation, and testing phases, even with incomplete climatic data. This makes it suitable for use in semi-arid regions like Mila, where data limitations are common.

The model is efficient, stable, and adaptable, offering a strong alternative to traditional methods. Although interpretability and parameter tuning remain challenges, the results confirm the model’s practical value in hydrology and agriculture.

In conclusion, the GRNN model provides a solid foundation for future research, and further improvements—such as automated tuning and regional validation—can enhance its scalability and real-world application.

General Conclusion

GENERAL CONCLUSION

This study has demonstrated the potential and effectiveness of using Generalized Regression Neural Networks (GRNN) as a data-driven approach to estimate reference evapotranspiration (ET_0) in the semi-arid context of Mila, Algeria. By leveraging limited climatic data and avoiding the strict assumptions required by traditional models such as the FAO Penman-Monteith equation, the GRNN model achieved outstanding predictive performance, with R^2 and NSE values exceeding 95%, and RMSE values below 0.4, across training, validation, and test datasets.

The developed model proved robust, efficient, and capable of capturing the nonlinear interactions between climatic variables—particularly under conditions of incomplete or inconsistent data. Its high agreement with reference values (e.g., WILSR ≈ 91%) and low relative error (≈ 4–5%) underscore its suitability for real-world applications in irrigation planning and water resource management.

One of the critical strengths of the GRNN approach lies in its adaptability. Unlike conventional empirical models, GRNN requires minimal parameter tuning and demonstrates strong generalization capability without overfitting. This is particularly beneficial for agricultural zones with scarce resources, where detailed meteorological monitoring is not always feasible.

Despite these promising outcomes, the study acknowledges several limitations. The lack of external validation with data from other regions and the manual nature of hyperparameter tuning represent areas for methodological improvement. Furthermore, while the model's accuracy is unquestionable, its interpretability remains limited—posing potential challenges in contexts that require transparent decision-making.

In conclusion, this research reinforces the role of artificial intelligence—particularly neural network models—in advancing sustainable agriculture under climate and resource constraints. The successful implementation of GRNN provides a scalable, replicable solution for ET_0 estimation, capable of enhancing precision irrigation and optimizing water usage. Future work is encouraged to explore hybrid AI approaches, integrate broader datasets, and validate the model across diverse agro-climatic zones to strengthen its generalizability and impact.

RECOMMENDATIONS

Based on the results obtained and the potential of Generalized Regression Neural Networks (GRNN) in modelling complex, non-linear relationships, the following recommendations are proposed for the effective application of GRNN in the Mila region:

1. Data Quality and Availability

To ensure optimal performance of the GRNN model, it is essential to use high-quality and comprehensive datasets. Continuous monitoring and collection of accurate meteorological and agricultural data (e.g., temperature, humidity, solar radiation, wind speed, and soil moisture) in the Mila region will significantly enhance model accuracy.

2. Local Calibration and Training

GRNN models should be trained using local data specific to the Mila region. Tailoring the model to regional conditions—such as crop type, soil characteristics, and climate patterns—improves its predictive capabilities and relevance.

3. Integration with Remote Sensing and GIS Tools

Integrating GRNN with remote sensing data and GIS tools can provide spatially distributed estimates of evapotranspiration (ET), enabling more precise irrigation planning and water resource management across the region.

4. Use for Irrigation Scheduling

The GRNN model can be effectively used to estimate daily or seasonal crop water requirements. This can support the development of dynamic, data-driven irrigation schedules, helping farmers optimize water usage and improve crop yields.

5. Model Updating and Validation

The GRNN model should be periodically updated and validated using the most recent data to maintain accuracy. Including diverse climatic years in the training dataset can also improve the model's generalization under changing weather conditions.

6. Capacity Building and Training

Local agricultural and water management stakeholders should be trained in the use of GRNN-based tools. Capacity building will facilitate adoption and long-term sustainability of advanced modelling practices.

7. Decision Support System Integration

GRNN outputs can be integrated into larger decision support systems (DSS) for agricultural planning, enabling more informed and proactive decision-making at both farm and regional levels.

8. Environmental Monitoring Applications

Beyond irrigation, GRNN can also be utilized in other applications such as drought monitoring, crop growth prediction, and assessment of climate change impacts in the Mila region.

Bibliographical references

Bibliographical references

[1] (https://dz.maptons.com/440862)

[2] Geographical map of Mila region (www.d-map.com, 2025)

[3] Ouaret & Drias (2020). *Problematic and Risks of Agricultural Activity in Fragile Environments*. Bulgarian Journal of Soil Science.

[4] Bendjouad (2023). *Estimating the Agricultural Production Function in the State of Mila*. Finance and Business Economics Review

[5] http://www.climate.gov.

[6] WeatherSpark. (n.d.). *Average Weather in Mila, Algeria Year Round*.

[7] The data presented in this section was gathered from reports issued by the National Agency for Water Resources (ANRH) in Algeria, as well as local studies on water management in the Mila region. For further details, refer to the agency's annual report (2022).

[8] Allen, R. G., Pereira, L. S., Raes, D., & Smith, M. (1998). *Crop evapotranspiration - Guidelines for computing crop water requirements*. FAO Irrigation and Drainage Paper No. 56

[9] Shiri, J., & Kisi, O. (2011). Comparison of genetic programming with neuro-fuzzy systems for modeling pan evaporation. *Hydrological Sciences Journal*, 56(5), 903–917.

[10] Traore, S., Kerh, T., Lin, Y. H., & Lu, M. H. (2010). Artificial neural network for modeling reference evapotranspiration complex process in arid regions. *International Journal of Biometeorology*, 54(1), 23–32.

[11] Chen, M., Yang, J., Saif, M., & Li, Y. (2009). Artificial neural network-based fault diagnosis methods: A review. In Fault Tolerant Flight Control (pp. 23–45). Springer.

[12] Specht, D. F. (1991). A general regression neural network. IEEE Transactions on Neural Networks, 2(6), 568–576.